UNIVERSITY OF TWENTE.

Faculty of Electrical Engineering,
Mathematics & Computer Science

Impact of the indoor propagation channel on a novel Bluetooth-compatible ranging method

Rowan A. de Vries
M.Sc. Thesis
June 1, 2018

Supervisors:
Prof. dr. ir. ing. F.B.J. Leferink
Dr. ir. J.C. Haartsen
Dr. ir. A. Meijerink
Z. Mahfouz, M.Sc.
Dr. ir. A.B.J. Kokkeler

Telecommunication Engineering Group
Faculty of Electrical Engineering,
Mathematics and Computer Science
University of Twente
P.O. Box 217
7500 AE Enschede
The Netherlands

Summary

An analysis is presented on the influence of multipath fading on the ranging method proposed by Haartsen [1]. The considered method uses the Bluetooth radio system, which has as advantage that the ranging method may in the future be added to the Bluetooth standard. The current standards for indoor ranging leave room for improvement. As such it is interesting to show how this method will be influenced by the indoor environments.

Typically indoor environments have many reflective paths a signal can travel by between transmitter and receiver. Therefore, the goal of this thesis is to determine the impact of multipath propagation on the ranging method's performance.

The impact of a multipath channel is shown analytically and verified by simulation. The performance is measured in the mean square error of the ranging estimate, including both noise and channel effects.

The theoretical background of the ranging method, which is a summary of [1], shows how the modulation of Bluetooth can be used for narrowband ranging, two-way time-of-flight measurements in an additive white Gaussian noise environment.

A stochastic channel model is presented for the indoor environment expected. For this a brief analysis of a deterministic channel model is shown and extended with average channel parameters. These parameters include the Rician K factor and delay spread. The analysis shows that the impact of multipaths on the ranging estimate can be seen as a weighted average of the different paths.

To validate the analysis a Simulink model is presented. The simulator follows all the steps from binary input of the RF modulator to the final distance estimate. A two-tap channel model is used to capture the delay dispersion caused by multipaths.

Using the simulator and the analysis, it is shown that they are in accordance with each other within the expected parameter ranges. The most noteworthy boundaries are the required signal-to-noise level, sampling frequency of the simulator and the delay spread.

Finally it is concluded that the ranging method requires a high K-factor and large signal-energy-to-noise ratio. The mean square error of the estimate relates roughly quadratically to the delay spread. This leads to undesirably high mean square errors for moderate delay spreads.

Contents

List of acronyms

ACF autocorrelation function

AWGN additive white Gaussian noise

BLE Bluetooth Low Energy

BT bandwidth time

CDF cumulative distribution function

FIR finite impulse response

GFSK Gaussian frequency shift keying

GMSK Gaussian minimum shift keying

LF low frequency

LOS line of sight

MP multipath

MSE mean square error

MSK minimum shift keying

NLOS non line of sight

PDP power delay profile

PLL phase locked loop

RF radio frequency

RMS root mean square

RSS received signal strength

RV random variable

SNR signal-to-noise ratio

TDD time division duplexing

ToF time of flight

TWToF two-way time-of-flight

WSS wide-sense stationary

WSSUS wide-sense stationary and uncorrelated scatterers

US uncorrelated scatterers

Chapter 1

Introduction

This thesis will show the impact of multipath channels on a novel ranging system compatible with Bluetooth Low Energy (BLE). The motivation for this work can be found in Section 1.1. The context and background for this research are provided in Section 1.2, followed by the scope of this work in Section 1.3. The goal of this research is presented in Section 1.4. The organisation of the thesis can be found in Section 1.5.

1.1 Motivation

There is a strong drive for the development of indoor localisation. For outdoors GPS has been around for decades and has found many applications, for instance, in navigation, tracking and gaming. However GPS does not work well indoors.

Currently the available indoor localisation methods face challenges [2]. Examples of current systems for indoor localisation are localisation based on Wi-Fi router connections and cameras. The former is typically accurate to a few meters, while the latter method leads to privacy concerns and it is expensive.

Localisation can be done by trilateration. This method uses the distance between location-known nodes and the node of interest. Many devices already have standardised radio systems for communication. These systems can also be used to determine the distance between devices.

1.2 Context

Jaap Haartsen has proposed a method to determine the distance between two radios utilising the existing Bluetooth radio system for ranging. In [1] a theoretical model for the system in additive white Gaussian noise (AWGN) is proposed and verified by experimental results.

Distance estimation methods, using radio frequency (RF) systems, are time of flight (ToF) and received signal strength (RSS). Direct ToF usually requires accurate synchronised clocks while RSS has major issues when operating in a reflective environment, such as indoors, making both impractical. The RSS will perform even worse for non line of sight (NLOS).

The method under investigation is based on a received phase difference of a signal caused by a round trip between radios [1]. One node transmits an RF signal, whose phase is modulated by an low frequency (LF) periodic signal. The second node transmits back the phase-locked signal, and the first node compares the received and transmitted instantaneous phases to determine the two-way time-of-flight (TWToF). The benefit of this TWToF method is that it does not have to synchronise clocks at the level required for ranging. Therefore, low-cost clocks can be used compared to regular ToF. In the future this system could be implemented in existing communication standards such as BLE.

Indoor environments can have many reflective paths for an RF signal to take between transmitter and receiver. Due to this, the transmitted signal arrives at the receiver from a different angle, with different phases, amplitudes and, angles of arrival. Even in a theoretical noiseless environment, the superposition of delayed versions of the signal may significantly disturb the ranging estimates.

The proposed method is similar to [3] in the sense that it uses TWToF and Bluetooth. However an extra correlation chip is used, which is not needed in [1]. A group of companies is going to provide services and devices based on a similar distance estimation method for Bluetooth [4], their exact methods are unknown to the author. This group of companies claims the method is very robust to multipath (MP) environments. The examples provided by the companies for potential applications seem to allow for long integration times and a strong line of sight (LOS).

Therefore, the next step in analysing the method under consideration, is to investigate the impact of MP effects.

1.3 Scope

This work is focused on the theoretical impact of MP effects for indoor environments. A theoretical analysis verified by simulations will be presented. As a measure of performance for the distance estimate, the mean square error (MSE) of the estimate will be shown. This will allow future system designers to make informed decisions on the influence of MPs on their link budget analysis. Implementation-specific properties are generalised in this work, except for properties provided by the BLE standard.

1.4 Objective

The aim of this research is to determine the impact of MP propagation together with AWGN on the ranging estimates performance in terms of the MSE. This will be studied analytically and verified by simulation.

1.5 Report organisation

A brief overview of the method under consideration is given in Chapter 2. In Chapter 3 the impact of MP effects is analytically evaluated including the distance estimate performance. The supporting simulation is presented in Chapter 4. A comparison of the analytic and simulated results is shown in Chapter 5. Following this, the conclusions and recommendations can be found in Chapter 6.

Chapter 2

Theory of the considered ranging method

The method proposed in [1] is summarised in this chapter. An overview of the method under consideration is presented in Section 2.1. The Bluetooth Gaussian frequency shift keying (GFSK) modulator can be used to generate a ranging symbol, as shown in Section 2.2. The relations between ToF, phase and distance are given in Section 2.3. Section 2.4 shows the demodulation and detection of the signal to get a distance estimate. Finally the performance with AWGN is shown in Section 2.5. Throughout this chapter and next chapter an explicit conditions list will be used to track the assumptions for which the analysis of the ranging method holds. The complete conditions list can be found in Appendix B

2.1 Overview ranging method

This section contains a condensed summery of the rest of this chapter. This summery provided the context in which the methods and analysis in the next sections are considered.

Ranging can be done using the BLE radio system. The total overview for the system as used in this work is given in Figure 2.1.

BLE uses a GFSK modulator with as input a bit series $B[k]$. The modulator generates a phase-modulated signal $s_{\mathrm{m}}(t)$ which is transmitted and delayed by the

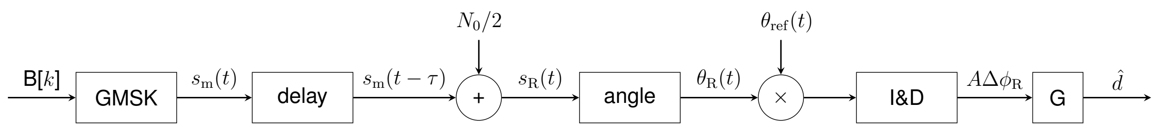

Figure 2.1: System overview. The symbols are explained in Section 2.1

round-trip time τ.

The received signal $s_{\mathrm{R}}(t)$ with modulated phase $\theta_{\mathrm{R}}(t)$ can be used to determine the phase shift caused by the time travelled, as explained in Section 2.4.

The detection uses a reference signal $\theta_{\mathrm{ref}}(t)$ and an integrate-and-dump operation. After integration the round-trip phase shift $\Delta\phi_{\mathrm{R}}$ with an extra gain A due to integration is found. Note that a number of conditions must be met, as discussed in the following sections, for this to be the case.

From this the distance estimate $\hat{d}$ can be computed by multiplication with a gain G, after which analysis of the distance estimate is possible.

2.2 GFSK signal generation

For a round trip of 300 m, the highest RF frequency which avoids phase ambiguity would be 1 MHz. Such a frequency is impractical as carrier frequency, as it requires large antennas. Therefore, the signal used for ranging will be an LF periodic phase-modulated signal as shown in Figure 2.2. BLE [5] uses a carrier frequency in the 2.4-GHz band and the information signal is modulated with GFSK. An overview of the related parameters is given in Table 2.1.

The GFSK modulator of Bluetooth can be used to generate an IQ baseband ranging signal whose instantaneous phase is close to a sinusoid. For TWToF an LF ranging signal is desirable in order to avoid phase ambiguity.

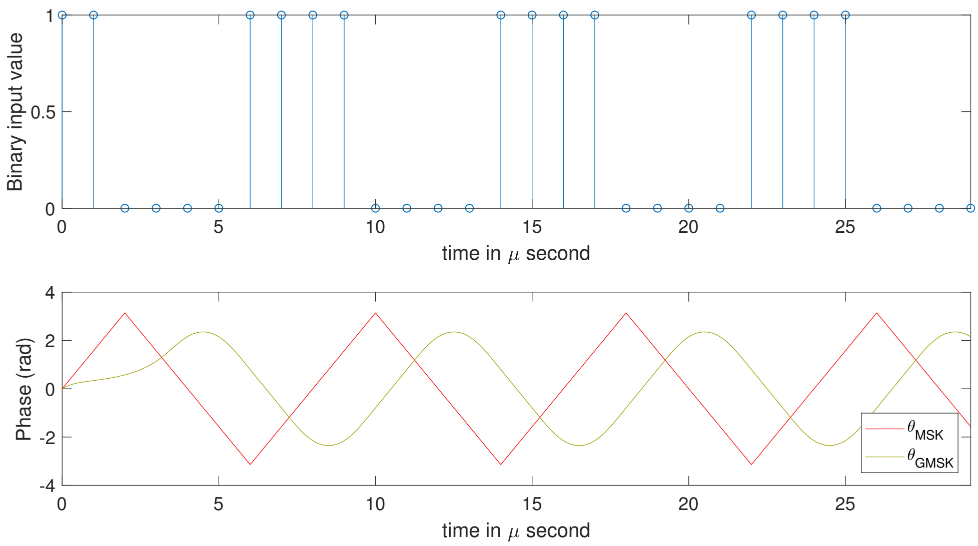

Figure 2.2: Top plot shows the bit sequence $B[k]$ input to the (G)MSK modulator. The bottom plot shows $\theta_{\mathrm{m}}(t)$ for MSK and GMSK modulation given the bit sequence input seen above.

Table 2.1: BLE and signal parameters

BLE parameters	**Symbol**	**Value range**
Carrier frequency	f_{c}	$2402 + 2k$ MHz, $0 \geq k \geq 39$
Bit rate	R_{BLE}	10^6 bps
Modulation depth	h	0.5 (no unit)
BT-product	BT	0.5 (no unit)
Signal parameters		
Signal frequency	f_{m}	$1/(2n)$ MHz, $n \in \mathbb{N}_{>0}$
Signal amplitude	A_{m0}	$2n/\pi$ radian

The modulation index of BLE is 0.5 so the modulation is effectively Gaussian minimum shift keying (GMSK). Therefore, a phase signal $\theta_{\mathrm{m}}(t)$ is generated with positive or negative slope of $\pi/2$ per bit time. By transmitting a bit sequence $B[k]$ of repeating number N of logical '1's followed by an equal number of '0's a triangular phase message signal is realised. For illustration Figure 2.2 shows what the signal would look like with and without the Gaussian filter. The frequency f_{m} and amplitude without Gaussian filtering A_{m} of this signal are

$$f_{\mathrm{m}} = \frac{R_{\mathrm{BLE}}}{2N}, \tag{2.1}$$

$$A_{\mathrm{m}} = \frac{N}{4}\pi, \tag{2.2}$$

where R_{BLE} is the bit rate of BLE, $R_{\mathrm{BLE}} = 10^6$ bits per second.

The bandwidth time (BT) product for the Gaussian filter is 0.5. Therefore, the signal gets a group delay of almost two bits and the sharp edges of the triangle will be smoothed. This effectively only passes the first harmonic, or first Fourier series coefficient, of the triangle, reducing the effective amplitude A_{m0} to

$$A_{\mathrm{m0}} = \frac{8}{\pi^2}A_{\mathrm{m}} \tag{2.3}$$

2.3 Two-way time-of-flight

The method used to determine the distance d is TWToF. In this system there are two nodes, A and B, that can actively communicate with each other. The interrogator (A) will send a ranging signal to the target (B) where the time travelled introduces a delay $\tau/2$. B will lock to the phase of the signal and store it in a phase locked loop (PLL) or instantly re-transmit the signal. When it is time to reply the ranging signal is sent back to A and the time travelled will introduce an extra delay $\tau/2$.

Therefore, the instantaneous phases at node B $\theta_{\mathrm{b}}(t)$ and the received signal at A $\theta_{\mathrm{R}}(t)$ are

$$\theta_{\mathrm{b}}(t) = \theta_m(t - \tau/2), \tag{2.4}$$

$$\theta_{\mathrm{R}}(t) = \theta_m(t - \tau), \tag{2.5}$$

where $\theta_m(t)$ is the transmitted message signal.

Extra delays will be introduced by nodes A and B, e.g. due to the Gaussian modulation filter. In this work these delays are considered stable and known such that they can fully be compensated for. Assuming stationary nodes this results in a total round-trip delay τ of

$$\tau = 2\frac{d}{c}, \tag{2.6}$$

where c is the speed of light.

The delay caused by the distance can be interpreted as a phase shift $\Delta\phi_{\mathrm{m}}$ of the transmitted signal

$$\Delta\phi_{\mathrm{m}} = 4\pi f_{\mathrm{m}}\frac{d}{c}, \tag{2.7}$$

The detected phase shift $\Delta\phi_{\mathrm{R}}$ will be slightly different from $\Delta\phi_{\mathrm{m}}$ due to noise and MP effects.

2.4 Signal detection

To estimate the distance $\hat{d}$ from the received signal $\tilde{s}_{\mathrm{R}}(t)$ three steps are taken, as shown in Figure 2.1. First the instantaneous phase of the received signal is calculated. In the second step the phase signal is multiplied by a reference signal with a $\pi/2$ phase offset, such that $\sin(\alpha)\cos(\beta) = 1/2(\sin(\alpha-\beta)+\sin(\alpha+\beta))$ results in the phase difference $\sin(\Delta\phi_{\mathrm{m}})$ and a term at twice the frequency. To linearise the expected phase difference must be small such that $\sin(\Delta\phi_{\mathrm{m}}) \approx \Delta\phi_{\mathrm{m}}$. Therefore,

$$d << \frac{c}{2f_{\mathrm{m,max}}} = 300 \text{ m}, \tag{2.8}$$

where $f_{\mathrm{m,max}}$ is 500 kHz. This leads to Condition 1. Note different detection methods could be used that do not need this requirement.

1. The round-trip distance should be small compared to $c/(2f_{\mathrm{m}})$.

Conditions list

To remove the double-frequency term, the third step is a lowpass filter. Using an integrate-and-dump operation over an integer number N_{int} of signal periods $1/f_{\mathrm{m}}$, or over a very large time, effectively cancels out the term at the double frequency and increases the desired signal power proportionally to the integration time. From 2.7 it follows that the distance estimate $\hat{d}$ is

$$\hat{d} = \frac{c\Delta\phi_{\mathrm{R}}}{4\pi f_{\mathrm{m}}}, \tag{2.9}$$

where $\Delta\phi_{\mathrm{R}}$ is the received phase difference. This difference is found by

$$\Delta\phi_{\mathrm{R}} = \frac{2}{A}\int_{t_0}^{t_0+N_{\mathrm{int}}/f_{\mathrm{m}}} \theta_{\mathrm{R}}(t)\theta_{\mathrm{ref}}(t)dt, \tag{2.10}$$

where $A = N_{\mathrm{int}}A_{\mathrm{m0}}/f_{\mathrm{m}}$, t_0 is the start time for the integrate and dump, $1/f_{\mathrm{m}}$ is the period of $\theta_{\mathrm{m}}(t)$, N_{int} is the number of signal periods per symbol, $\theta_{\mathrm{R}}(t)$ is the received signal and $\theta_{\mathrm{ref}}(t)$ is $\theta_{\mathrm{m}}(t)$ with a $\pi/2$ phase offset.

2.5 Performance in AWGN

This section reuses the result for the MSE of the distance estimate due to AWGN from [1] and explains its use in this work. For this work it is assumed that the target node introduces no error to the signal, Condition 2. This reduces the complexity of the system. Condition 1 must apply and, for the ranging method to work, the carrier power must be significantly larger than the noise power, Condition 3.

2. The target node introduces no error to the signal.
3. The noise power at the detector input is small compared to the RF carrier power $A_{\mathrm{c}}^2/2$.

Conditions list

It can be shown that the complex noise can be decomposed in a part parallel and a part perpendicular to the complex carrier. The parallel part mainly influences the amplitude and is not of interest when Condition 3 applies. The noise perpendicular to the RF amplitude results in phase errors as shown in Figure 2.3. With these assumptions it can be shown that the MSE of the distance estimate $\sigma_{\mathrm{d_n}}^2$ and for GMSK $\sigma_{\mathrm{d_n,GMSK}}^2$ are

$$\sigma_{\mathrm{d_n}}^2 = \frac{c^2}{4}\frac{1}{4\pi^2 f_{\mathrm{m}}^2 A_{\mathrm{m}}^2}\frac{1}{E_{\mathrm{s}}/N_0}, \tag{2.11}$$

$$\sigma_{\mathrm{d_n,GMSK}}^2 = \frac{c^2}{16}\frac{T_{\mathrm{b}}^2}{E_{\mathrm{s}}/N_0}, \tag{2.12}$$

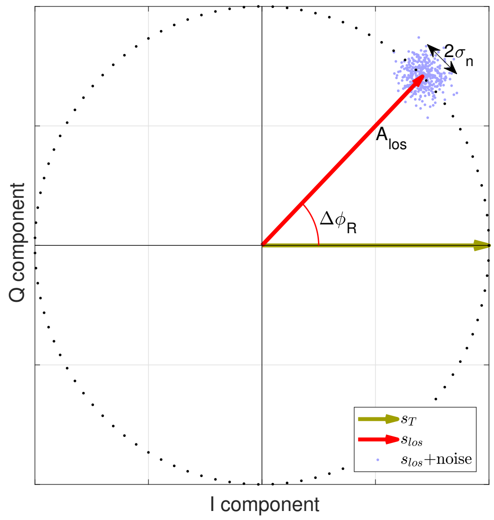

Figure 2.3: Visualisation of $s_{\mathrm{R}}(t)$ in complex envelope of transmitted signal $s_{\mathrm{m}}(t)$, with AWGN around the received signal indicating possible realisations.

where E_{s}/N_0 is the signal-to-noise ratio (SNR) per symbol, T_{b} is the bit time, f_{m} is given by (2.1) and A_{m0} is given by (2.3).

For the given application of BLE the bit time T_{b} is set to 1 μs. Therefore, the noise contribution to the MSE of the distance estimate only depends on E_{s}/N_0.

The SNR per symbol is a function of the noise spectral density N_0 and the symbol energy

$$E_{\mathrm{s}} = \frac{1}{2} A_{\mathrm{c}}^2 |H(0)|^2 T_{\mathrm{s}}, \tag{2.13}$$

where A_{c} is the carrier amplitude, $|H(0)|^2$ is the total DC power transfer of the channel and T_{s} is the symbol time.

The symbol time is determined by the integrate and dump operation

$$T_{\mathrm{s}} = N_{\mathrm{int}} T_{\mathrm{m}} \tag{2.14}$$

where N_{int} is the number of periods over which is integrated.

To determine $A_{\mathrm{c}}^2/2$ a full link budget analysis should be done for a given implementation.

Chapter 3

Analysis of multipath effects

This chapter presents channel models to analyse MP effects and show their impact on the ranging estimate. It starts with a general description of MPs in Section 3.1, followed by a description of a basic discrete-rays model in Section 3.2. Building up to a stochastic model the expected RF environment is presented in Section 3.3. For this environment, the discrete-ray model is extended to a stochastic model in Section 3.4. The quality of the distance estimate will be expressed in the MSE of the distance estimate as presented in Section 3.5. An indication of what happens if the target node does make errors is shown in Section 3.6. The mathematical derivation of the channel models and MSE is shown in Appendix A.

For compact writing and calculation, without loss of generality, signals are represented as equivalent-baseband signals. With this representation both the RF and the LF phases and amplitudes are fully described. Following the representation as in 'Introduction to analog & digital communications' [6]. Equivalent-baseband signal are designated by a tilde. Therefore, a modulated wave $s(t)$ can be expressed in terms of its equivalent-baseband representation $\tilde{s}(t)$ as

$$s(t) = s_{\mathrm{I}}(t)\cos(2\pi f_{\mathrm{c}}t) - s_{\mathrm{Q}}(t)\sin(2\pi f_{\mathrm{c}}t) = \mathrm{Re}\left\{\tilde{s}(t)e^{j2\pi f_{\mathrm{c}}t}\right\} \tag{3.1}$$

where f_{c} is the carrier frequency, $s_{\mathrm{I}}(t)$ and $s_{\mathrm{Q}}(t)$ are respectively the in-phase and quadrature-phase components of the modulated wave.

3.1 Multipaths

In free space, a transmitted signal can only reach a receiver by one path, the LOS. If one reflector is added then there are two paths the signal can take to reach the receiver. The analysis of such a situation is done in Section 3.2. The left side of Figure 3.1 shows a possible realisation of the LOS, one MP and the resulting received signal in the complex envelope of the transmitted signal. The phase and

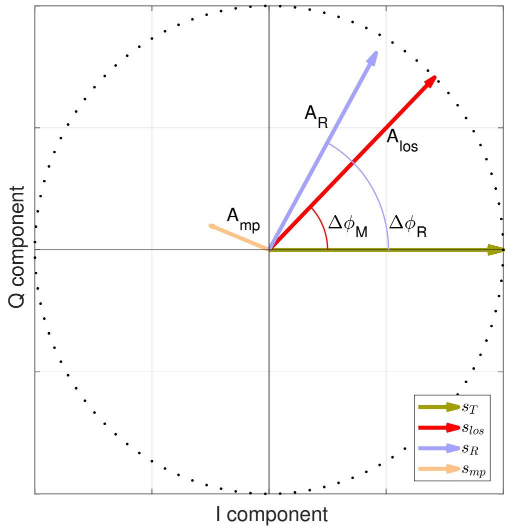

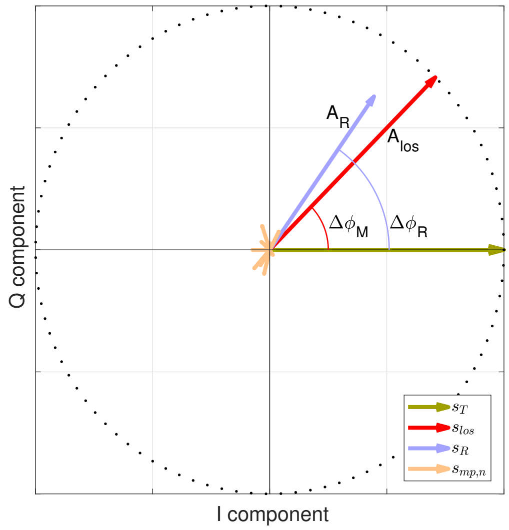

Figure 3.1: Visualisation of $s_{\mathrm{LOS}}(t)$ and $s_{\mathrm{R}}(t)$ in complex envelope of transmitted signal $s_{\mathrm{m}}(t)$ with 1 MP in the left figure and 10 MPs on the right.

magnitude of the MPs are examined in Section 3.3. The received signal is the complex sum of the LOS and MP components. Both the amplitude and phase of the received signal can therefore change in comparison to the LOS. This continues to hold true for multiple MPs as can be seen on the right side of Figure 3.1. Both figures show a reduction in amplitude and additional phase shifts; this does not have to be the case. MPs can have either a positive or a negative impact on both the phase difference and the amplitude.

The amplitude of the received signal is of importance because the signal power determines the SNR in (2.12). If the phases of the MPs are random then on average they will cancel out and have little influence on the LOS amplitude, assuming a large SNR.

The phase change has a direct impact on the estimated phase difference, causing a channel-dependent error in the distance estimate. It is therefore important to know if and when the channel realisation changes. A more thorough analysis is presented in Sections 3.2 and 3.4.

3.2 Discrete ray channel model

If there are different paths the transmitted signal can take to reach the receiver, then knowing the attenuation, phase shift and delay of each path fully describes a linear channel.

For the N-ray model, the equivalent-baseband channel impulse response $\tilde{h}(t)$ is

$$\tilde{h}(t) = \sum_{i=1}^{N} a_i \delta(t - \tau_i), \tag{3.2}$$

where N is the total number of paths, a_i and τ_i are the complex amplitude and the group delay for each ray, respectively, and $\delta(\cdot)$ is the Dirac delta function.

In Subsection 3.3.3 it will be shown that the phase shift caused by the excess delays of MPs is small compared to 2π. The group delay of each path causes both an RF and LF phase shift, only the LF phase shift is relevant here. This assumption is necessary for the impact of the MPs to be linearised.

4. The phase shift caused by the excess delays of MPs is small, $2\pi f_{\mathrm{m}} \tau_{ex} << 2\pi$.

Conditions list

With Condition 4, it is shown in Appendix A.1 that the received phase signal $\theta_{\mathrm{R}}(t)$ can be approximated as

$$\begin{aligned} \theta_{\mathrm{R}}(t) &= \arg\left\{\tilde{s}_{\mathrm{R}}(t)\right\} \\ &= \arg\{A\} + \sum_{i=1}^{N} \theta_{\mathrm{m}}(t - \tau_i)\, \mathbb{R}\mathrm{e}\left\{\frac{a_i}{A}\right\} + N_{\mathrm{Q}}(t), \end{aligned} \tag{3.3}$$

where $N_{\mathrm{Q}}(t)$ is the AWGN contribution and A is the total complex amplitude of the channel,

$$A = \sum_{i=1}^{N} a_i. \tag{3.4}$$

From this it can be seen that the contribution of each path to the distance estimate is a weighted average over all components. It is good to note that this is significantly different than the time-of-arrival method used by wide-band estimation methods. The $\arg\{A\}$ contribution is static and will drop out during the phase difference detection. It can be seen that a large phase signal will occur when A comes close to zero, this even can happen with only strong components due to their phase.

To show the impact of a single MP the special case of two ray of which one is the LOS component and one is the MP is given as example.

For the equivalent-baseband channel response

$$\tilde{h}(\tau) = a_{\mathrm{los}}\delta(t - \tau_{\mathrm{los}}) + a_{\mathrm{mp}}\delta(t - \tau_{\mathrm{los}} - \tau_{\mathrm{ex}}), \tag{3.5}$$

where a_{los} is the amplitude of the LOS component, τ_{los} is the group delay of the LOS, a_{mp} is the complex amplitude of the MP component, and τ_{ex} is the excess delay of the MP component.

Under Conditions 1, 2 and 3, (2.7) and (3.3) can be used to estimated the distance $\hat{d}$. This is calculated from the received phase $\Delta\theta_{\mathrm{R}}$ as follows

$$\hat{d} = \frac{c}{2}\left(\mathbb{R}\mathrm{e}\left\{\frac{a_{\mathrm{los}}}{a_{\mathrm{los}} + a_{\mathrm{mp}}}\right\}\tau_{\mathrm{los}} + \mathbb{R}\mathrm{e}\left\{\frac{a_{\mathrm{mp}}}{a_{\mathrm{los}} + a_{\mathrm{mp}}}\right\}(\tau_{\mathrm{los}} + \tau_{\mathrm{ex}})\right) + d_{\mathrm{n}}, \tag{3.6}$$

where d_{n} is the noise contribution to the distance estimate. From this, the mean and MSE are seen to be

$$\mathrm{E}[\hat{\mathrm{d}}] = d_{\mathrm{los}} + d_2, \tag{3.7}$$

$$\begin{aligned}\mathrm{MSE}[\hat{\mathrm{d}}] &= d_2^2 + \sigma_{d_{\mathrm{n}}}^2 \\ &= \left(\frac{c}{2}\mathbb{R}\mathrm{e}\left\{\frac{a_2}{a_{\mathrm{los}} + a_2}\right\}\tau_{\mathrm{ex}}\right)^2 + \sigma_{d_{\mathrm{n}}}^2,\end{aligned} \tag{3.8}$$

where $\sigma_{d_{\mathrm{n}}}^2$ is given by (2.12).

Therefore, the impact of the MP is inversely related to the power of the LOS component. If both a_{los} and a_{mp} are equivalent in strength, but opposite in sign then the distance estimated can attain any value within one wavelength of f_{m}. During such a fading dip ranging should not be done. This result can be seen as an addition to the two-path model presented in [1], in which the phase change due to the angle of reflection was not considered.

This deterministic channel model will be extended to a stochastic channel model in Section 3.4. To that end, the following section will provide insight into the stochastic properties of an indoor channel for the considered ranging method.

3.3 Channel properties

This section will provide the bases for the stochastic channel model presented in Section 3.4. Starting with wide-sense stationary and uncorrelated scatterers (WSSUS) assumptions in Subsection 3.3.1. The importance of a LOS is presented in Subsection 3.3.2. The power delay profile (PDP) and coherence bandwidth for an indoor channel are presented and analysed in Subsections 3.3.3 and 3.3.4 respectively.

3.3.1 Wide sense stationary and uncorrelated scatterers (WSSUS)

Following the definitions in 'Wireless Communications' [7] two important assumptions are made about the channel. It is wide-sense stationary (WSS) and has uncorrelated scatterers (US).

A zero mean channel is WSS if the autocorrelation function (ACF) of the channel response does not depend on time t and a later time t' but only on the difference $t-t'$. Generally, this is not true over long time intervals as a moving node faces changes of the statistical channel due to shadowing and variations in path loss. For this work an even stricter assumption is made, the channel is static within each measurement.

The channel has US when "contributions with different delays are uncorrelated" [7]. This is valid if the phase of a MP contains no information about another MP.

5. The channel is US and quasi static.

Conditions list

3.3.2 Line-of-sight (LOS)

LOS channels can be characterised by the Rician K factor

$$K = \frac{P_{\mathrm{LOS}}}{P_{\mathrm{MPs}}}, \tag{3.9}$$

where P_{LOS} is the power in the LOS component and P_{MPs} is the power in the MP components.

As the angle of reflection adds an extra phase shift to the signal, the relation between phase and the distance traveled by a reflected signal becomes ambiguous. This is advantageous to the ranging method under consideration, as MPs will give a zero-mean phase contribution. Therefore, in WSSUS channels only a dominant component can be used for distance estimation as all other contributions cancel out on average.

A dominant component can occur in a NLOS situation, in that case the derivations remain valid. However the distance estimate will have an expected value of the distance traveled by the dominant path, which for NLOS is not the distance between the nodes.

6. There must be a dominant component in the channel for the ranging method to work.

Conditions list

3.3.3 Power delay profile and excess delays

The PDP represents the statistically expected power as a function of excess delay τ_{ex}. Equivalently, the PDP could be expressed in delay τ shifted by τ_{los}, but this provides no extra insight.

The root mean square (RMS) delay spread is a measure for the delay dispersion in a channel. For indoor environments, the RMS delay spread is typically 5-10 ns for residential buildings and 5-100 ns for office environments [7]. BLE has 1 MHz RF bandwidth. Therefore, the excess delay times expected are small compared to the sampling time. Therefore, a dense PDP $P_{\mathrm{h}}(\tau_{\mathrm{ex}})$ model can be used, Condition 7. A typical example of a PDP is

$$P_{\mathrm{h}}(\tau_{\mathrm{ex}}) = \begin{cases} \frac{1}{\sigma_\tau} e^{-\tau_{\mathrm{ex}}/\sigma_{\tau,\mathrm{dif}}}, & \text{if } \tau_{\mathrm{ex}} \geq 0 \\ 0, & \text{otherwise} \end{cases} \tag{3.10}$$

where $\sigma_{\tau,\mathrm{dif}}$ is the RMS delay spread of the diffuse channel, so excluding a LOS. The PDP is normalised to make it independent of the total power transfer. The power transfer includes losses such as path loss and shadowing, which are effectively modeled in the E_{s}/N_0.

A distinction is made between the RMS delay spread of the diffuse channel $\sigma_{\tau,\mathrm{dif}}$ and the RMS delay spread of the total channel including a LOS σ_τ. A possible realisation of a total channel could be (3.10) with a delta peak at zero for the LOS.

MPs have two contributions to the phase shift, one caused by the reflection and another caused by the time travelled. The reflection only impacts the RF phase, while the time traveled gives a group delay. For later linearisation it is important to note that the phase shifts due to the excess delay τ_{ex} are related as

$$\phi_{\mathrm{mp},\tau_{\mathrm{ex}}} \approx 2\pi f_{\mathrm{m}} \tau_{ex}. \tag{3.11}$$

As $f_{\mathrm{m}} <$ 500 kHz and $\sigma_\tau \leq$ 100 ns the phase shift due to the excess delay time is small, $\phi_{\mathrm{mp},\tau_{\mathrm{ex}}} << 2\pi$.

7. The channel has a dense exponential PDP.

Conditions list

3.3.4 Coherence bandwidth

The coherence bandwidth is a measure for the band of frequencies over which the channel response is the same, or flat. This has two applications for the ranging method. The first application is to verify if the frequency response over the RF bandwidth of BLE is flat. The second application is to verify if successive measurements, which use frequency hopping, have uncorrelated channel realisations.

The calculations for the coherence bandwidth are taken from [7]. The coherence bandwidth B_{coh} can be found from the frequency correlation function $R_{\mathrm{H}}(\Delta f)$. The frequency correlation function is the Fourier transform of the PDP, for (3.10)

$$R_{\mathrm{H}}(\Delta f) = \mathcal{F}\left\{P_{\mathrm{h}}(\tau)\right\} = \frac{1}{1 + j2\pi\Delta f \sigma_\tau}, \tag{3.12}$$

where Δf is the frequency deviation and $\mathcal{F}\{\cdot\}$ is the Fourier transform.

The correlation bandwidth B_{coh} is equal to Δf when $|R_{\mathrm{H}}(\Delta f)|$ reaches half its maximum value

$$\frac{|R_{\mathrm{H}}(\Delta f)|}{\max(|R_{\mathrm{H}}(\Delta f)|)} = 0.5. \tag{3.13}$$

Therefore, the coherence bandwidth is

$$B_{\mathrm{coh}} = \frac{\sqrt{3}}{2\pi\sigma_\tau} \tag{3.14}$$

For the expected range of the RMS delay spread this leads to a maximum coherence bandwidth of 55 MHz, and a minimum of 2.8 MHz. Therefore, with 1 MHz RF bandwidth flat fading can be assumed.

It is advantageous to averaging out the effect of the channel on the ranging estimate if the channel realisations are uncorrelated. BLE uses frequency hopping over a range of 80 MHz, with 2 MHz spacing between channels. This means that it cannot be assumed that the frequency hopping will always result in uncorrelated channel realisations. However time division duplexing (TDD) is used. Therefore, the temporal behaviour of the channel in combination with frequency hopping is likely to make the channel realisation uncorrelated for each ranging symbol.

The parameters to apply from the coherence bandwidth are shown in Table 3.1. It can be concluded that flat fading over the 1 MHz RF bandwidth can be assumed. However, the assumption that each channel realisation will be independent from the previous realisation, is a simplification that does not always hold for BLE.

Table 3.1: Overview channel and BLE parameters

Channel parameters	Symbol	Value range
RMS delay spread	σ_τ	5-100 ns
Coherence bandwidth	B_{coh}	2.8-55 MHz
BLE parameters		
RF bandwidth		1 MHz
Hopping range		80 MHz
Minimum hopping distance		2 MHz

3.4 Stochastic channel model

This section aims to explain the usage and interpretation of the stochastic channel model. The derivation is provided in Appendix A.

The results of Section 3.2 can be generalised from discrete rays to continuous time contributions. The equivalent-baseband channel is $\tilde{h}(t)$.

From this it can be shown that the received signal is given by,

$$\tilde{s}_{\mathrm{R}}(t) = A_{\mathrm{c}} e^{\mathrm{j}\theta(t)} \tilde{H}(0) \left\{ 1 + \frac{\mathrm{j}}{\tilde{H}(0)} \int \tilde{h}(\tau) \left[\theta(t-\tau) - \theta(t) \right] \mathrm{d}\tau \right\} + N(t), \quad (3.15)$$

$$\arg\left\{\tilde{s}_{\mathrm{R}}(t)\right\} \approx \arg\left\{\tilde{H}(0)\right\} + \int \theta(t-\tau) \,\mathbb{R}\mathrm{e} \left\{ \frac{\tilde{h}(\tau)}{\tilde{H}(0)} \right\} \mathrm{d}\tau + \frac{N_{\mathrm{Q}}(t)}{A_{\mathrm{c}} |\tilde{H}(0)|}, \quad (3.16)$$

$$|\tilde{s}_{\mathrm{R}}(t)| \approx A_{\mathrm{c}} |\tilde{H}(0)|, \quad (3.17)$$

where A_{c} is the carrier amplitude, $\theta(t)$ is the modulating signal, $N_{\mathrm{Q}}(t)$ is the quadrature component of the noise, $|\cdot|$ is the magnitude, $\mathbb{R}\mathrm{e}\{\cdot\}$ is the real part of the complex value and $\tilde{H}(f)$ is the equivalent baseband transfer function of the channel,

$$\tilde{H}(f) = \int \tilde{h}(\tau) e^{-j2\pi f \tau} \mathrm{d}\tau. \quad (3.18)$$

An important observation is that the contributions to the phase estimates are a weighted average over all contributing parts, equivalently to (3.3).

For a strong LOS, $K >> 1$, it can be seen that the total amplitude of the channel response becomes almost fully deterministic

$$\mathrm{E}\{\tilde{H}(0)\} \approx a_{\mathrm{los}} \quad (3.19)$$

$$\mathrm{E}\{|\tilde{H}(0)|^2\} \approx |a_{\mathrm{los}}|^2 \frac{1+K}{K}. \quad (3.20)$$

Therefore, $\tilde{h}(\tau)/\tilde{H}(0)$ becomes a linear operation of a Gaussian $\tilde{h}(\tau)$ and, almost, deterministic $\tilde{H}(0)$. For low K values this term cannot be assumed to have a Gaussian distribution.

8. There must be a strong LOS $K >> 1$ for the ranging estimate to be Gaussian.

Conditions list

After detection it can be shown that

$$\hat{d} = d + d_{\mathrm{h}} + d_{\mathrm{n}}, \tag{3.21}$$

where d is the actual distance, d_{h} is the channel contribution and d_{n} is the contribution due to noise.

$$d = \frac{c}{2}\tau_{\mathrm{LOS}}, \tag{3.22}$$

$$d_{\mathrm{h}} = \frac{c}{2}\int \mathbb{R}\mathrm{e}\left\{\frac{\tilde{h}_{\mathrm{MPC}}(\tau)}{\tilde{H}(0)}\right\}(\tau - \tau_{\mathrm{LOS}})d\tau, \tag{3.23}$$

$$d_{\mathrm{n}} \sim \mathcal{N}\left(0, \frac{c^2 N_0}{8\pi^2 f_{\mathrm{m}}^2 A_{\mathrm{m}}^2 A_{\mathrm{c}}^2 |\tilde{H}(0)|^2 T_{\mathrm{s}}}\right). \tag{3.24}$$

Both d_{h} and d_{n} are assumed to be zero mean. Therefore, the estimate will be unbiased,

$$\mathrm{E}[\hat{\mathrm{d}}] = \mathrm{d}. \tag{3.25}$$

3.5 Mean square error (MSE)

The performance of the distance estimation is expressed in the MSE, or variance. The derivations are provided in Appendix A.4, under Conditions 1-8.

The MSE σ_{d}^2 of the distance estimate consists of two parts, one due to the MPs and one due to the AWGN:

$$\sigma_{\mathrm{d}}^2 = c^2\left[\frac{\sigma_{\tau,\mathrm{dif}}^2 + T_{\mathrm{m,dif}}^2}{8K} + \frac{T_{\mathrm{b}}^2}{16E_{\mathrm{s}}/N_0}\right], \tag{3.26}$$

where $\sigma_{\tau,\mathrm{dif}}^2$ and $T_{\mathrm{m,dif}}^2$ are, respectively, the RMS delay spread and the mean excess delay of the diffuse part of the channel. Both are related to the PDP, in this case excluding the LOS.

In general, the RMS delay spread σ_τ and mean excess delay T_m are

$$\sigma_\tau^2 = \frac{\int P_\mathrm{h}(\tau_\mathrm{ex})\tau_\mathrm{ex}^2 d\tau_\mathrm{ex}}{P_\mathrm{m}} - T_\mathrm{m}^2, \tag{3.27}$$

$$T_\mathrm{m} = \frac{\int P_\mathrm{h}(\tau_\mathrm{ex})\tau_\mathrm{ex} d\tau_\mathrm{ex}}{P_\mathrm{m}}, \tag{3.28}$$

where $P_\mathrm{h}(\tau_\mathrm{ex})$ is the PDP and P_m is the total channel power transfer.

For exponential PDPs, $T_\mathrm{m,dif} = \sigma_{\tau,\mathrm{dif}}$. With this it can be shown that σ_τ is related to its diffuse versions as

$$\sigma_\tau^2 = \frac{1+2K}{(1+K)^2}\sigma_{\tau,\mathrm{dif}}^2. \tag{3.29}$$

So (3.30) can be rewritten as

$$\sigma_\mathrm{d}^2 = c^2\left[\sigma_\tau^2\frac{(1+K)^2}{4K(1+2K)} + \frac{T_\mathrm{b}^2}{16E_\mathrm{s}/N_0}\right]. \tag{3.30}$$

For large K this is approximately

$$\sigma_\mathrm{d}^2 \approx c^2\left[\frac{\sigma_\tau^2}{8} + \frac{T_\mathrm{b}^2}{16E_\mathrm{s}/N_0}\right]. \tag{3.31}$$

From this analysis it follows that the impact of MPs is mostly dependent on the σ_τ^2. The assumption throughout this work has been a strong dominant component, if this is the case then the MSE is almost not effected by K.

An important observation is that the AWGN contribution is not influenced directly by the MP channel.

From Appendix C it follows that for communication a E_b/N_0 of approximately 10 dB is needed. The equivalent SNR per symbol is

$$E_\mathrm{s}/N_0 = nE_\mathrm{b}/N_0, \tag{3.32}$$

where n is the number of BLE bits per ranging symbol.

3.6 Impact of errors in the target node on the MSE

This section will add the impact of noise added by the target and consequently model the channel twice. Until now only going through the channel and noise at the receiver of the interrogator were considered where the channel was describing the full round-trip channel.

The target node will use a PLL to store the modulating phase before transmitting back to the interrogator. The detection method in PLLs can use a multiplication with a $\pi/2$ phase off-set signal to lock to the signal. With this assumption, it is roughly equivalent to the detection used in the interrogator. Therefore, a similar phase estimation error will be made as in the interrogator.

BLE uses TDD and fast frequency hopping. Therefore, it is expected that the channel realisation from the interrogator to the target and the channel realisation back are different. However it is assumed that, if there is no shadowing, the channel statistics do not change.

With AWGN at the target and assuming the two channels are travelled by, it can be seen that effectively two errors are made. One error caused by the channel from interrogator to target and the AWGN at the target and another by the return channel with AWGN in the interrogator. As the errors are independent

$$\begin{aligned}\sigma_{\mathrm{d}}^2 &\approx c^2\left[\frac{\sigma_\tau^2}{8} + \frac{T_{\mathrm{b}}^2}{16E_{\mathrm{s,t}}/N_0} + \frac{\sigma_\tau^2}{8} + \frac{T_{\mathrm{b}}^2}{16E_{\mathrm{s,i}}/N_0}\right] \\ &= c^2\left[\frac{\sigma_\tau^2}{4} + \frac{T_{\mathrm{b}}^2}{16E_{\mathrm{s,t}}/N_0} + \frac{T_{\mathrm{b}}^2}{16E_{\mathrm{s,i}}/N_0}\right], \end{aligned} \tag{3.33}$$

where $E_{\mathrm{s,t}}$, $E_{\mathrm{s,i}}$ are the symbol energies at the target and interrogator respectively.

On the other hand, if the same channel realisation is used for both transmissions then the error caused by the channel is doubled. Therefore, the variance due to the channel gets quadrupled compared to (3.31)

$$\sigma_{\mathrm{d}}^2 \approx c^2\left[\frac{\sigma_\tau^2}{2} + \frac{T_{\mathrm{b}}^2}{16E_{\mathrm{s,t}}/N_0} + \frac{T_{\mathrm{b}}^2}{16E_{\mathrm{s,i}}/N_0}\right]. \tag{3.34}$$

The next chapter will focus on providing a simulator to verify the simpler case, excluding errors in the target.

Chapter 4

Implementation simulator

The simulator follows the same structure as presented in Chapter 2. The order of the sections is from signal generation to distance estimate. The channel is implemented with a two-tap model, as presented in Section 4.4. The simulator is implemented in Mathworks Matlab and Simulink version R2017b.

The simulator is built up as in Figure 4.1. Using Condition 2 (error-free target), only the interrogator and channel have influence on the ranging performance. Tables with the parameter values for each Simulink block will be presented, and non-reported parameters remain at the default values.

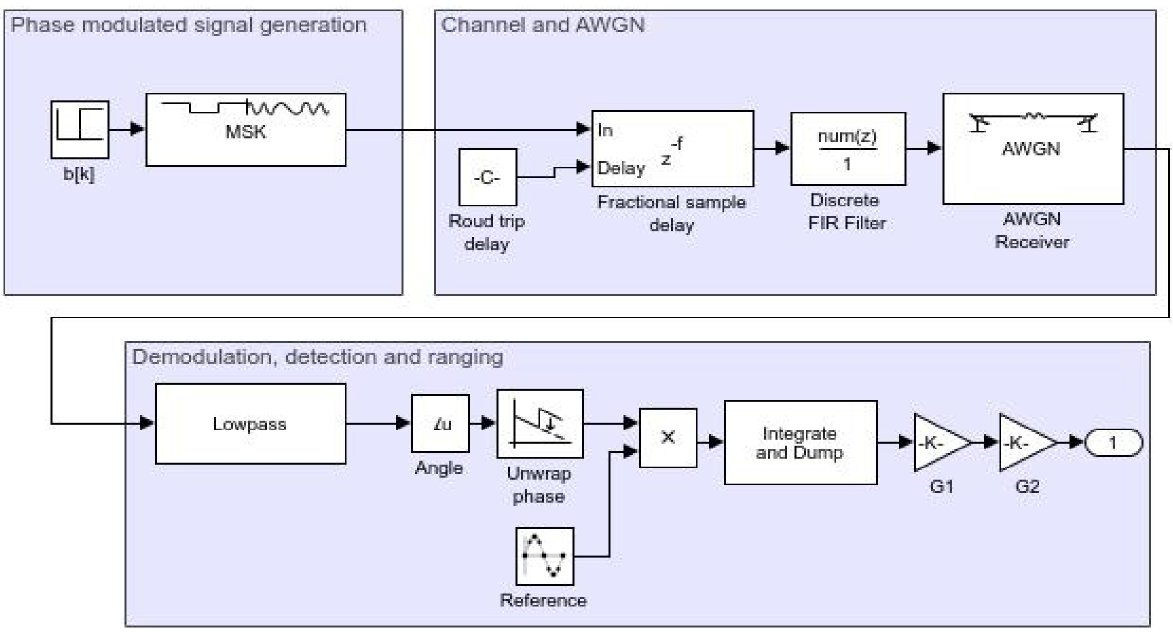

Figure 4.1: Overview simulator implementation in Simulink.

4.1 Bit stream

The bit stream $b[k]$ is used to create a cosine-shaped modulated phase. A logical '1' creates a positive slope in the instantaneous phase and a logical '0' a negative slope. As such, the bit stream should start with '0's to go down for half the modulation time, followed by '1's such that the phase modulating signal goes up for the second half of the modulation time.

The bit rate is 1 Mbps. A total of 40 bits per modulation period are used, resulting in a modulation frequency of 25 kHz as reported in Table 4.1.

Table 4.1: Simulation parameters, bit stream

Bit stream parameters	**Symbol**	**Value range**
Bit rate	R_{BLE}	1 Mbps
Bit time	T_{B}	1 μs
Bits per period	$2N$	40 bits
Modulation frequency	f_{m}	25 kHz
Simulink block		**Sample time output**
Repeating Sequence Stair		1/R_{BLE} seconds

4.2 Modulator

A minimum shift keying (MSK) baseband modulator is used instead of the GMSK modulator. Using an GMSK modulator would result in an extra delay due to the filter and changes the shape of the signal, approximately reducing the amplitude as in (2.3). The delay could be compensated for.

The amplitude reduction is implemented by using a sinusoidal reference signal for detection instead of a triangular signal. This makes the effective modulation amplitude A_{m0} independent of the mismatch between a pure cosine and the GMSK modulated signal. The mismatch between the GMSK modulated signal and the cosine increases for a lower modulation frequency f_{m} as only the tips are rounded. For extremely low f_{m} the straight sides of the triangle will at some point become dominant over the smoothing effect over the top in 2 bit times.

The MSK modulator can use one sample per bit. The complex baseband fully describes the system. However using more samples per bit N_{MSK} results in a finer sampling grid, which has benefits for the simulator distance estimate performance as shown in Section 5.1. Therefore, an oversampling of 16 will be used.

The other settings are given in Table 4.2.

Table 4.2: Simulation parameters, modulator

Modulator parameters	**Symbol**	**Value range**
Samples per MSK symbol	N_{MSK}	16 samples
Input type		Bit
Rate options		Allow multirate
Simulink block		**Sample time output**
MSK Modulator Baseband		$T_{\mathrm{B}}/N_{\mathrm{MSK}}$ seconds

4.3 Round-trip delay

The delay is implemented using a filter-based fractional delay block. The delay in samples N_{frac} is

$$N_{\mathrm{frac}} = \frac{dN_{\mathrm{MSK}}}{cT_{\mathrm{B}}}, \tag{4.1}$$

where d is the round-trip distance, N_{MSK} is the number of MSK samples per bit, c is the speed of light and T_{B} is the bit time.

The delay uses a linear interpolation between samples. This is an approximation of what would happen in reality. Due to the bandwidth truncation, sampling can be seen as convolution with a sinc function in the time domain. Therefore, a more accurate result should be achieved by using a re-sampled sinc with more terms. For this work the linear interpolation is sufficiently accurate as will be shown in Section 5.1.

The round-trip distance d_{r} and number of samples per MSK symbol N_{MSK} will be varied. As $0 < d_{\mathrm{r}} < 40$ m, $N_{\mathrm{MSK}} \leq 16$, the range of the fractional delay in samples will be $0 < N_{\mathrm{frac}} < 2.14$. Leading to the simulator settings in Table 4.3.

Table 4.3: Simulation parameters, fractional delay

Delay parameters	**Symbol**	**Value range**
Samples delay	N_{frac}	0< N_{frac} <3 samples
Round-trip distance	d_{r}	0< d_{r} ≤40
Simulink blocks		**Sample time output**
Constant		$T_{\mathrm{B}}/N_{\mathrm{MSK}}$ seconds
Variable Fractional Delay		$T_{\mathrm{B}}/N_{\mathrm{MSK}}$ seconds

4.4 Two-tap model

In general a tapped-delay-line $h(t)$ can be described as

$$h(t) = \sum_{n=1}^{N} c_n \delta(t - n\Delta T) \tag{4.2}$$

where ΔT is the sampling time, N is the number of taps and c_n is the complex coefficient per delay.

In a tapped-delay-line model, the effects of all signal paths that arrive within one tap are summed up. The statistics within a tap will not change due to Condition 5 (US and quasi-static). The first tap b_1 contains the LOS and MPs and thus has Rician fading. Later taps $b_{n>1}$ only contain MPs and will therefore be Rayleigh fading.

4.4.1 Sampling time

Assuming an exponential PDP (3.10), the received power will on average decrease with increasing delays. When almost all MP power is received in the first two taps, within sampling time $2\Delta T$, the signal dispersion is only significantly influenced by the MP power in the second tap. Later taps have decaying impact, so for large sampling times their impact can be neglected. For ($\sigma_\tau << \Delta T$) only two taps are needed, Condition 9. If the RMS delay spread is not small compared to the sampling time, then it is necessary to add more taps to the model.

9. The two-tap simulation model requires $\sigma_\tau << \Delta T$.

Conditions list

4.4.2 Parameters two-tap model

Three parameters are needed to describe the two-tap model with LOS. These are the LOS power A^2_{LOS}, the power of the MPs in the first tap $2\sigma_1^2$ and the power of the MPs in the second tap $2\sigma_2^2$. The MP power in the taps is given as $2\sigma_n^2$ because they are complex Gaussian variables.

The A^2_{LOS}, $2\sigma_1^2$ and $2\sigma_2^2$ parameters can be expressed in the Rice factor K, the RMS delay spread σ_τ and normalised channel power.

In the analysis, the propagation loss will not be considered along with the multipath propagation, but modeled separately. As a consequence the total average power of the multipath channel is normalised to one as in

$$A_{\mathrm{los}}^2 + 2\sigma_1^2 + 2\sigma_2^2 = 1. \tag{4.3}$$

Using the definition of the Rice factor (3.9)

$$K = \frac{A_{\mathrm{los}}^2}{2\sigma_1^2 + 2\sigma_2^2} \tag{4.4}$$

the power of the LOS can be expressed as

$$A_{\mathrm{los}}^2 = \frac{K}{K+1}. \tag{4.5}$$

The RMS delay spread σ_τ is related to the PDP and mean delay spread T_{m} as in (3.27) and (3.28), where the total channel power P_{m} is 1 due to normalisation. As the first tab has $\tau_{\mathrm{ex}} = 0$, the RMS delay spread is fully described by the second tap. The excess delay in the second tap equals the sampling time ΔT. Therefore,

$$\sigma_\tau^2 = (2\sigma_2^2 - 4\sigma_2^4)(\Delta T)^2, \tag{4.6}$$

$$\sigma_2^2 = \frac{1 - \sqrt{1 - 4\frac{\sigma_\tau^2}{\Delta T^2}}}{4} \approx \frac{\sigma_\tau^2}{2(\Delta T)^2}. \tag{4.7}$$

From the channel normalisation it can be seen that the power in of the MPs in the first tap must be

$$\sigma_1^2 = \frac{1 - 2\sigma_2^2 - A_{\mathrm{los}}^2}{2} \approx \frac{1 - \sigma_\tau^2/(\Delta T)^2 - A_{\mathrm{los}}^2}{2} \tag{4.8}$$

4.4.3 Implementation

The two-tap model is implemented as a finite impulse response (FIR) filter with two coefficients c_1 and c_2. The first coefficient uses (4.5) and (4.8), while c_2 is given by (4.7). Therefore,

$$c_1 \sim \mathrm{c}\mathcal{N}(A_{\mathrm{los}}, 2\sigma_1^2), \tag{4.9}$$

$$c_2 \sim \mathrm{c}\mathcal{N}(0, 2\sigma_2^2), \tag{4.10}$$

where $\mathrm{c}\mathcal{N}(\mu, \sigma^2)$ is the complex normal distribution with mean μ and variance σ^2, leading to the setting for the FIR filter as in Table 4.4.

Table 4.4: Simulation parameters, two-tap model

Two-tap parameter	**Symbol**	**Value range**
Coefficients	c_1, c_2	vector with tap coeff.
Simulink block		**Sample time output**
Discrete FIR Filter		$T_\mathrm{B}/N_\mathrm{MSK}$ seconds

4.5 AWGN

For the noise model to be valid, Conditions 2 and 3 must hold. There is a straightforward block to use for AWGN. The block can be used in SNR per symbol or SNR per bit mode. The difference in SNR is

$$SNR_\mathrm{s} = k\, SNR_\mathrm{b}, \tag{4.11}$$

where k is the number of bits per symbol.

The symbol time T_s is determined by the integrate and dump operation. Therefore, it can be seen from (2.10) that

$$T_\mathrm{s} = N_\mathrm{int}/f_\mathrm{m}, \tag{4.12}$$

where the number of symbol periods to integrate N_int will be 1 in most cases as this reduces the simulation time.

When the simulator does not use 1 MHz sampling frequency for the noise block, a bandwidth restriction can be added by a lowpass filter. The impact of the lowpass filter will be discussed in Section 5.2. The setting used in this work is a passband from 0-1 MHz and a stopband from 3 MHz with 80 dB suppression. This leads to a delay of 14 samples which must be compensated for in the reference signal.

The setting used are shown in Table 4.5.

4.6 Demodulation, detection and ranging

This section follows the theory from Section 2.4.

The signal of interest is phase modulated. Therefore phase detection is needed. As the instantaneous phase is wrapped by 2π an extra step is needed to unwrap the signal. Both steps are available as Simulink blocks.

Table 4.5: Simulation parameters, AWGN

AWGN parameters	**Symbol**	**Value range**
Initial seed		randomised integer
Mode		Es/N0
Es/N0		$E_\mathrm{s}/N_0 > 30$ dB
Symbol period	T_s	
Passband edge frequency		1 MHz
Stopband edge frequency		3 MHz
Simulink block		**Sample time output**
AWGN Channel		$T_\mathrm{B}/N_\mathrm{MSK}$ seconds
Lowpass filter		$1/N_\mathrm{MSK}$ seconds

The multiplication by a reference sinusoidal signal, with frequency f_m and unit amplitude, and the integration step are straightforward operations.

The output of the integrate and dump operator will be multiplied by a constant G_1 as in (2.10), resulting in $\sin(\Delta\theta_\mathrm{R})$. The gain to get the $\sin(\Delta\theta_\mathrm{R}) \approx \Delta\theta_\mathrm{R}$ term is

$$G_1 = \frac{2}{2NN_\mathrm{MSK}A_\mathrm{m0}}. \tag{4.13}$$

From the phase difference the distance is calculated as in (2.9) by a multiplication G_2 of

$$G_2 = \frac{c}{4\pi f_\mathrm{m}} \tag{4.14}$$

The complete settings are presented in Table 4.6.

Table 4.6: Simulation parameters, demodulation, detection and ranging

Ranging parameters	**Symbol**	**Value range**
Modulation frequency	f_m	25 kHz
Integration period	T_s	$>$40 μs
Gain from integration to phase	G_1	
Gain from phase to distance	G_2	
Simulink blocks		**Sample time output**
Sine Wave		$T_\mathrm{B}/N_\mathrm{MSK}$ seconds
Product		$T_\mathrm{B}/N_\mathrm{MSK}$ seconds
Integrate and Dump		T_m seconds
Gain(2x)		T_m seconds

Chapter 5

Results of the simulation vs analysis

In this chapter the comparison of the simulation with the analysis is presented. In Section 5.1 the accuracy of the simulator is shown. In Section 5.2 the minimum SNR required for the analysis to be valid is presented. The impact of the K-factor and delay spread are shown in Section 5.3. The overall results for MPs and AWGN effects on the ranging method are presented in Section 5.4. The cumulative distribution function (CDF) of the distance estimate can be used to calculate outage probabilities and show the distribution in general. In this work the CDFs are not analysed. Appendix D shows the CDFs for a most of cases presented in this chapter.

Throughout this chapter confidence intervals of 95% are shown. A distinction is made between the confidence interval for the distance estimate and its MSE. However for both cases the confidence interval shown is only valid for Gaussian distributions.

For the distance estimates the confidence interval CI_d is

$$CI_d = \bar{d} - Q^{-1}(0.25)\frac{s_d}{\sqrt{n}}, \bar{d} + Q^{-1}(0.25)\frac{s_d}{\sqrt{n}}, \tag{5.1}$$

where $Q^{-1}(\cdot)$ is the inverse Q-function, $\bar{d}$ is the sample mean, s_d is the sample standard deviation and n is the number of independent ranging symbol realisations.

For the MSEs the confidence interval CI_{σ^2} presented is only valid for Gaussian distributions

$$CI_{\sigma^2} = \frac{ns^2}{\mathrm{i}\chi_n^2(0.975)}, \frac{ns^2}{\mathrm{i}\chi_n^2(0.025)}, \tag{5.2}$$

where $\mathrm{i}\chi_n^2(\cdot)$ is the inverse cumulative Chi squared distribution for n degrees of freedom.

5.1 Simulation error

In order to investigate the accuracy of of the simulator, the simulator is validated without MPs and AWGN. From Figure 5.1 it can be seen that there is a distance dependant error $\hat{d}_{\mathrm{err}}$. The error is found by subtracting the simulated distance and the real distance $\hat{d}_{\mathrm{sim}} - d$.

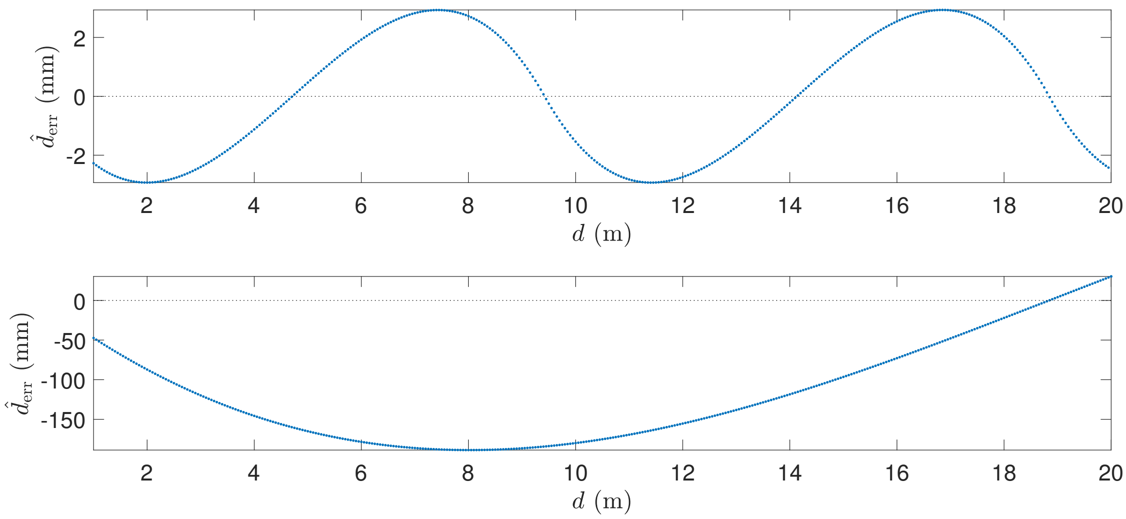

Figure 5.1: Simulation error due to fractional delay, no AWGN or MPs. **Top:** 16 MHz sampling. **Bottom:** 4 MHz sampling.

The error depends on the sampling frequency f_{s}, as shown for 4 MHz and 16 MHz. The error is likely to be a consequence of the linear interpolation fractional delay block or caused by rounding errors.

For a 4 MHz sampling frequency the maximum error has a magnitude of 189 mm and a periodicity over 37.5 m. Over the range of interest this results in a large simulation error that is mostly a negative contribution to the estimate. This is not desirable.

For a 16 MHz sampling frequency the performance is much better. The maximum error is 2.9 mm with a periodicity over 9.4 m. Therefore, over the range of interest there are both positive and negative contributions, both with a small impact on the total result.

If a higher simulation precision is needed, then either a better implementation must be found for the fractional delay, or the sampling frequency must be further increased. The downside of increasing the sampling frequency is that more intermediate data is generated, resulting in a longer simulation time. The ranging data would not change as that is only dependent on the amount of ranging symbols simulated.

5.2 Minimum requirement SNR

For the noise it is important to note that Condition 3 (high SNR) is relevant to the ranging method analysis, but not problematic to the simulator. The analysis does not work for low SNR because the RF carrier is not large enough, compared to the noise. Due to this both the in-phase and quadrature-phase parts of the noise become relevant. Moreover, the MSE of the distance estimate rises so high that the ranging method becomes unusable. As the problem is related to the carrier-to-noise ratio the problem cannot be solved by longer integration times.

The analytic relation between the SNR and MSE of the distance estimate (2.12) is expected to hold under Condition 3. Two scenarios are presented, first what without a bandwidth restriction and next with the lowpass filter described in Section 4.5.

From the simulation the limiting cases for the SNRs are shown in Figure 5.2. This shows that the theoretical curve from the analysis matches the simulated MSE from an E_b/N_0 of approximately 23 dB. Note that this very high and can be reduced by adding a lowpass filter.

For the 40 of bits per symbol used throughout this work, the equivalent E_s/N_0 with an integration over one period $N_\mathrm{int} = 1$, is 39 dB. If the symbol time is increased with $N_\mathrm{int} = 10$, then the minimum required E_s/N_0 is also shifted by 10 dB.

The consequences of the minimum SNR can be mitigated somewhat by intelligently combining multiple ranging estimates, for instance by ignoring distance estimates larger than 100 meters.

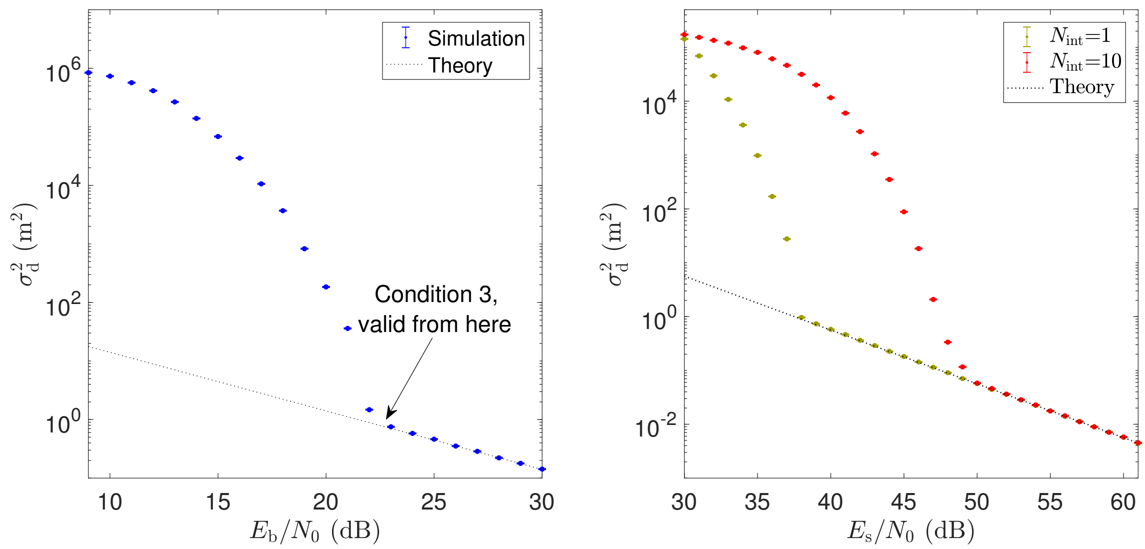

Figure 5.2: SNR vs MSE indicating valid range model without lowpass-filter, the MSE over 20.000 ranging symbols is taken.
Left: SNR per bit equivalent, **Right:** SNR per symbol, for different T_s

With the addition of a lowpass filter the E_b/N_0 matches the same theoretical curve (2.12) from 14 dB, as can be seen in Figure 5.3. A stricter filter could somewhat move the breaking point to even lower E_b/N_0.

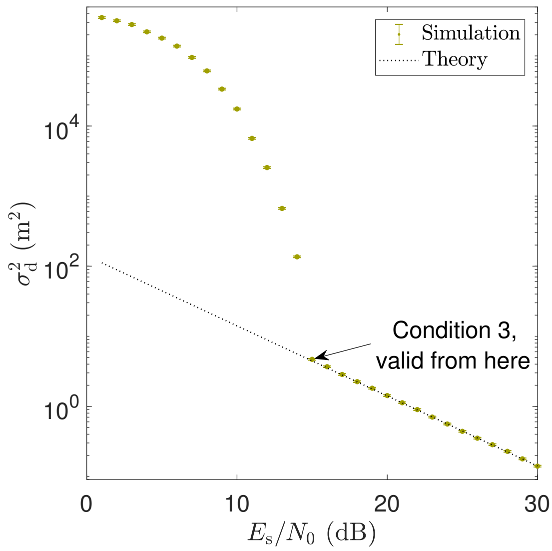

Figure 5.3: SNR per bit vs MSE indicating valid range model, the MSE over 10.000 ranging symbols is taken.

Regardless of the filter used there is a lower limit to the SNR with respect to the carrier. As a consequence, the integration time for a ranging signal has an upper limit and the detectable E_s/N_0 a minimum. For the experiment above that limit is

$$(E_\mathrm{s}/N_0)_\mathrm{min} = (E_\mathrm{b}/N_0)_\mathrm{min} N\mathrm{int} \approx 25 N\mathrm{int} \tag{5.3}$$

5.3 Delay spread and K-factor

For high K-factors the MSE is related only to the delay spread. To verify this three scenarios are presented. For each example independent simulations are run,

1. 1000 symbols with $\sigma_\tau = 2$ ns and $E_\mathrm{s}/N_0 = 44$ dB,
2. 1000 symbols with $\sigma_\tau = 2$ ns and $E_\mathrm{s}/N_0 = 47$ dB,
3. 1000 symbols with $\sigma_\tau = 3$ ns and $E_\mathrm{s}/N_0 = 44$ dB.

Two effects are expected from theory (3.30) and (2.13). For a low K-factor the channel power transfer $|H(0)|^2$ becomes more random. Due to this the E_s for some realisations will drop below the required threshold described in the previous section. When the noise is not the limiting factor (3.30) should hold. Note that the impact of the MP on the distance estimate becomes non-Gaussian for low K values. Therefore, strictly speaking, the confidence interval shown in the results is based on a false assumption for low K.

In Figure 5.4 the simulation results are presented. On the left side it can be seen that the theoretical curve and the simulated results do not match for low K-factors, while the right shows that is does hold for large K-factors. Due to the limited number of symbols the result of experiment 1 at a K of 10 is seen to be off significantly. However this is not generally the case.

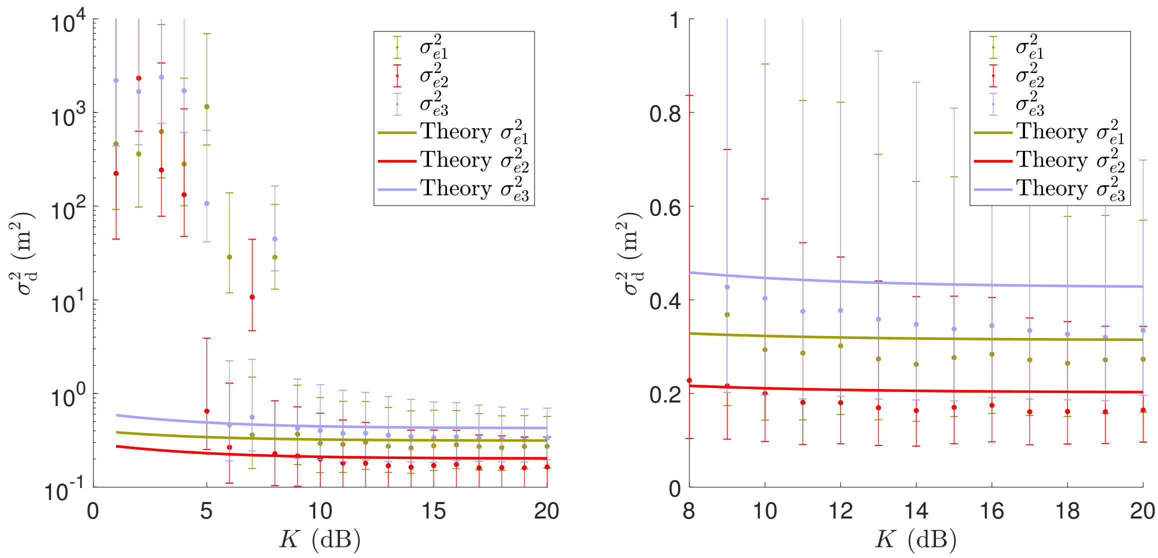

Figure 5.4: Impact K-factor for three different σ_τ, E_s/N_0 values, where σ_1^2, σ_2^2 and σ_3^2 are the MSEs of, respectively, experiments 1, 2 and 3.
Left: K-factor over a large range with logarithmic y scale,
Right: K-factor for large K on a linear y scale

The impact of the excess delay time is tested separately. For a high K-factor it is expected that the MSE of the distance estimate (3.31), is only depending on the excess delay time. This is verified by the experiment simulated, without noise and with K=100.

Figure 5.5 shows that the simulator and analysis are only comparable for small values of σ_τ. For an MSE of 0.25 m^2, $\sigma_\tau < 5$ the error between theory and simulation is insignificant.

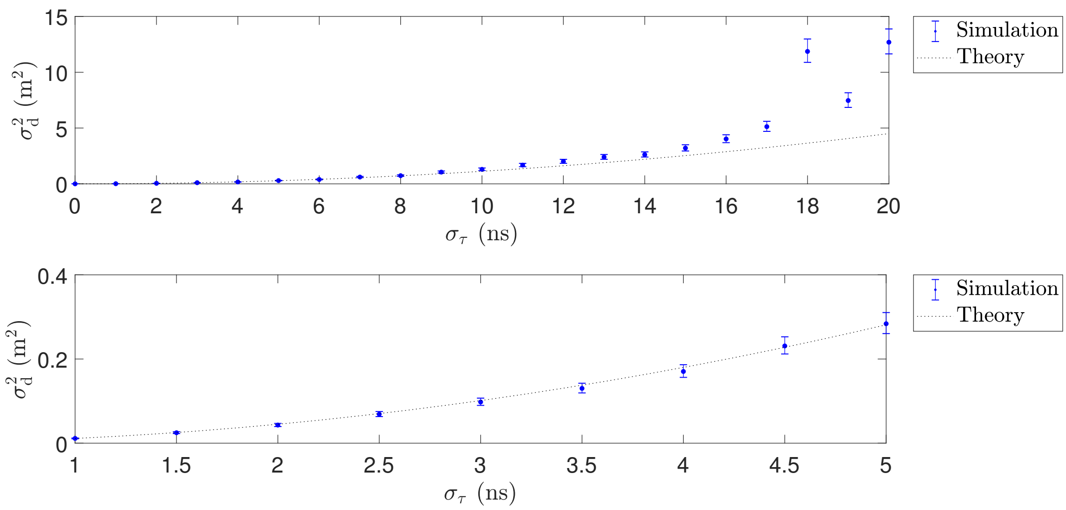

Figure 5.5: RMS delay spread vs MSE of the ranging estimate, without noise.
Top: Large RMS delay spread range.
Bottom: RMS delay spread in range of interest.

5.4 Verification total model

In this section it is shown that the analysis is in accordance with the simulation for the valid range of $E_{\rm b}/N_0$, K, σ_τ and d. This will be done by working out an example case in four experiments. First the the MSE as a function of the number of ranging samples used is presented in three experiments. Later a final experiment demonstrates the overall distance estimate behavior.

An interesting limit to show is when the MSE of the ranging estimate remains just below 0.25 m^2. From (3.31) it can be seen that the overall expected MSE is the sum of σ_h^2 and $\sigma_{\rm n}^2$.

To this end an $E_{\rm s}/N_0 = 47$ dB of will be used. From (2.12) this results in a $\sigma_{\rm n}^2$ equal to 0.112 m^2. For the MP contribution a σ_τ of 3 ns results in a $\sigma_{\rm h}^2$ of 0.102 m^2.

Therefore the expected MSE $\sigma_{\rm d}^2$ is

$$\sigma_{\rm d}^2 = \sigma_{\rm n}^2 + \sigma_{\rm h}^2 = 0.214 \text{ m}^2. \tag{5.4}$$

For this example three independent simulations are run as validation,

1. 5000 symbols with only AWGN, $E_{\rm s}/N_0 = 47$ dB,
2. 5000 symbols with only MP effects, $K = 100,\ \sigma_\tau = 3$ ns,
3. 5000 symbols with both AWGN and MP effects as above.

The estimated MSE at n samples $\sigma^2_{\mathrm{d},n}$ is

$$\hat{\sigma}^2_{\mathrm{d},n} = \frac{1}{n}\sum_{i=1}^{n}(\hat{d}_i - d)^2 \tag{5.5}$$

where $\hat{d}_i$ is the distance estimate of simulated ranging symbol i and n is the number of symbols used to calculate the MSE. The resulting MSEs are shown in Figure 5.6.

For the first simulation an E_s/N_0 of 47 dB without MP effects is run. From the figure it follows that the predicted MSE is reached.

In the second simulation the two-tap model parameters a K-factor of 100 (linear) and an RMS delay spread σ_τ of 3 ns. For each of the 1000 symbols a new randomly generated channel realisation is used. In this manner it is shown that the MSE due to MPs indeed converges to the predicted value.

In the third experiment both AWGN and MP effect as described above are included. From this it can be seen that the addition of the MSEs caused by AWGN and MPs does indeed describe the MSE of the total ranging estimate.

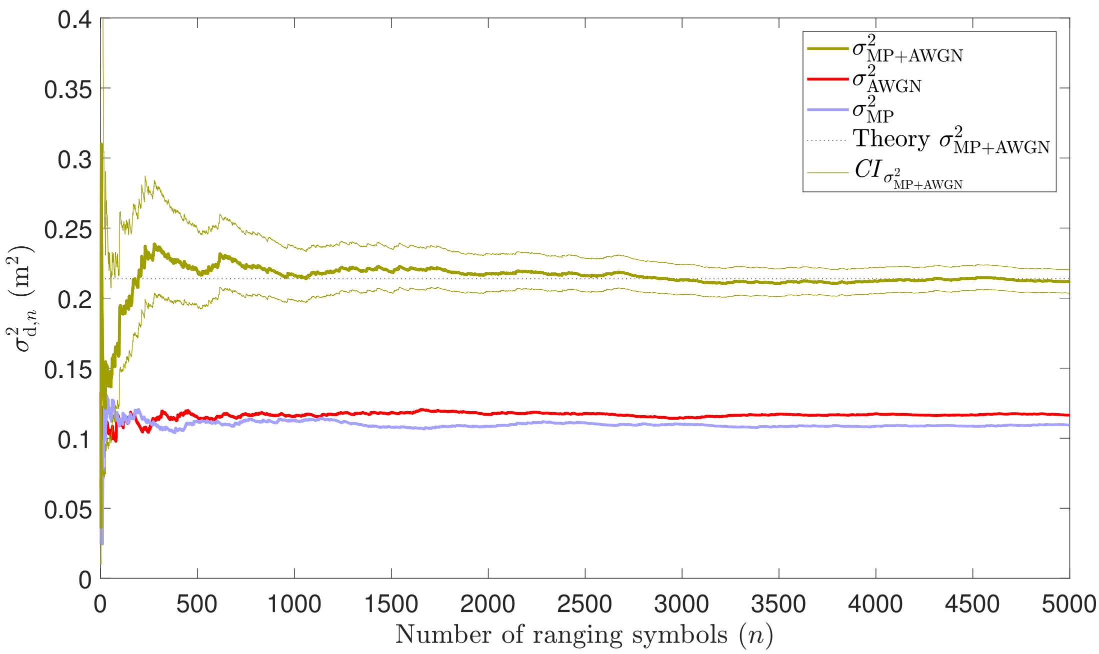

Figure 5.6: Development of the MSE as a function of the number of samples used to determine it.

As the main goal of ranging is distance estimation the next experiment will show this estimation. In this experiment the distance is stepped from 1 m to 20 m with constant $E_\mathrm{s}/N_0 = 47$, $K = 100$ and $\sigma_\tau = 3$ ns for 2000 independent channel realisations. From (3.7) and (3.31) it can be seen that the distance error should be unbiased and its MSE should be independent of the distance. Note that this is only the case as the E_s/N_0, K and σ_τ do not change. In a physical setting these depend on the distance.

In Figure 5.7 the total performance of this experiment is shown. From multiple of such experiments it is concluded that the distance estimate statistics do not depend directly on the distance.

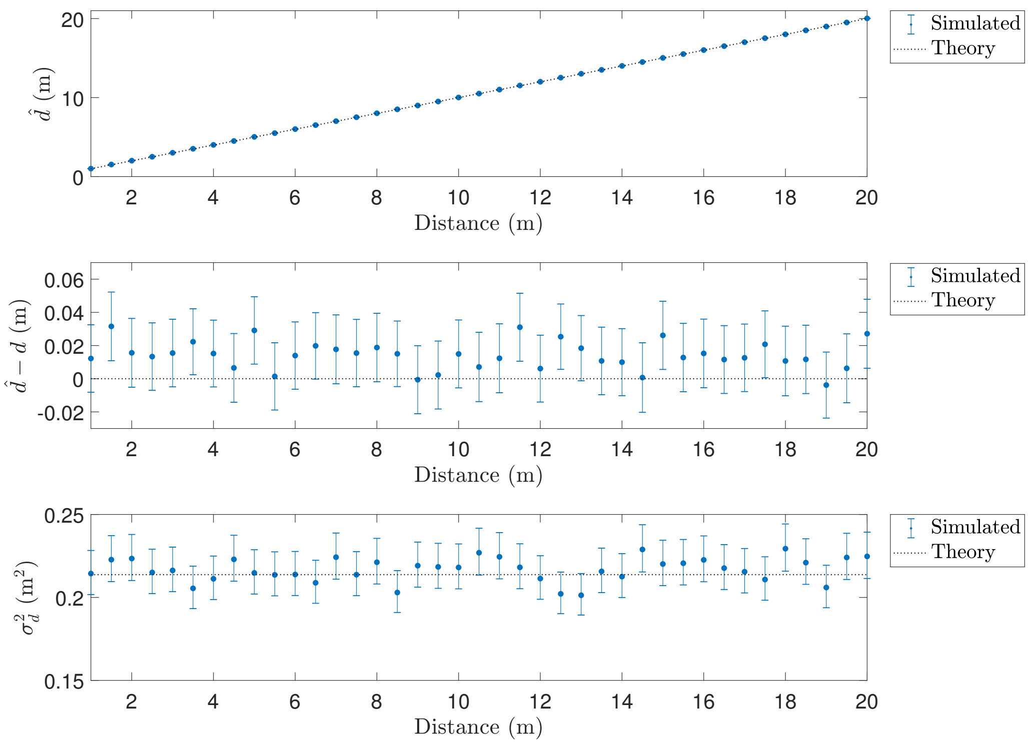

Figure 5.7: Distance estimation over 20 m. **Top:** Distance vs distance estimate **Middle:** Distance vs estimation error. **Bottom:** Distance vs MSE.

Chapter 6

Conclusions and recommendations

The conclusions of this report are presented in Section 6.1. For future work the recommendations are presented in Section 6.2.

6.1 Conclusions

From the first chapter: ”The aim of this research is to determine the impact of MP propagation together with AWGN on the ranging estimates performance in terms of the MSE.”

In this report it is shown that the overall performance, in terms of the MSE, is well approximated by the sum of the MSE due to the channel and the MSE due to the noise. However for this result to be valid the conditions used throughout this work must apply. These conditions are listed in Appendix B.

For the considered ranging method to work a dominant path must be available for the signal to travel by. When this is the case an estimation can done for the length of this path. In most cases the dominant path is the LOS, which contains the information desired for ranging.

An interesting observation is that the impact of MPs can be seen as a weighted average over their contribution to the distance estimate. This is different than wide-band methods that use the first received component for their estimate.

The MSE of the distance estimate due to MPs scales approximately quadratically with the RMS delay spread for high K-factors. As a consequence the ranging method will only perform well in environments with small delay spreads and a strong LOS. Only a quasi-static environment was considered. The performance would increase if the channel produces more independent errors within one ranging symbol, provided the phase detection can handle it.

By simulation it is shown that the minimum equivalent SNR per bit equivalent required for the ranging method has an impact on the maximum integration time.

This puts an upper limit on the symbol energy that can be gathered for a given SNR.

Based on the findings presented in the report it is expected that the ranging method will work for indoor environments, as long as there is a strong LOS component, low delay spread and a high SNR.

6.2 Recommendations

In this section three recommendations are made. One related to the channel model, one related to validation of the presented work and one on combining ranging data.

In this work a quasi-static channel is assumed. It would be interesting to see the impact of a time-varying channel on the ranging method, in particular as the ranging can use a considerable amount of time to improve the SNR.

It would be interesting to see the analysis and simulation presented in the work validated by an experiment. Such an experiment could work as the experiment presented in [1], repeated in different environments with known channel characteristics.

When intelligently combining ranging data, a significant improvement of the MSE can be expected. The most basic form would be outlier detection for low E_b/N_0. A different type of combining ranging data is sensor fusion. The distance estimate is approximately Gaussian for a strong LOS. Therefore, its statistics are fully described by the mean and variance, making it relatively easy to incorporate in sensor fusion acquired by different means.

Bibliography

[1] J. Haartsen, A. Stek, F. Hooijschuur, and T. Hulshof, “Narrowband RF distance measurement using phase locked FM transceivers,” in *2016 Symposium on Communications and Vehicular Technology (SCVT)*. IEEE, 2016, pp. 1–6.

[2] Z. Farid, R. Nordin, and M. Ismail, “Recent advances in wireless indoor localization techniques and system,” *Journal of Computer Networks and Communications*, 2013.

[3] G. Fischer, B. Dietrich, and F. Winkler, “Bluetooth indoor localization system,” *Proceedings of the 1st workshop on positioning, navigation and communication*, 2004.

[4] “Imec sets new benchmark with 30cm accurate and secure localization solution based on bluetooth,” cached IMEC website news article. [Online]. Available: https://webcache.googleusercontent.com/search?q=cache:HxVDfJWAYc0J:https://www.imec-int.com/en/articles/imec-sets-new-benchmark-with-30cm-accurate-and-secure-localization-solution-based-on-bluetooth+&cd=1&hl=nl&ct=clnk&gl=nl

[5] “Bluetooth core specification version 5.0,” *Specification of the Bluetooth System*, 2016.

[6] S. Haykin and M. Moher, *An introduction to analog and digital communications*, 2nd ed. John Wiley & Sons, 2007.

[7] A. F. Molisch, *Wireless communications*, 2nd ed. John Wiley & Sons, 2012.

[8] W. C. Van Etten, *Introduction to random signals and noise*. John Wiley & Sons, 2006.

Appendix A

Derivation of channel response to phase and distance estimates

This appendix contains mathematical derivations for the impact of MP effects under the condition that phase changes, caused by time traveled, are small compared to 2π and there is a large SNR. Effectively this limits the derivation to LOS scenarios. In Section A.1 the impact of discrete rays on the detected phase and magnitude of the received signal is derived. The result of this derivation is generalised in Section A.2 to have continuous-time contribution instead of discrete rays. Using the theory from Chapter 2 and the continuous-time channel response the impact of the modulation, detection and noise is derived in Section A.3. The impact of a stochastic channel model is presented in Section A.4.

The text and mathematics in the text are the interpretations of the author.
The mathematical derivations and equations are the work of A. Meijerink.

A.1 Discrete ray channel impulse response effect on phase estimate

Assuming a channel response with discrete ray contributions as in (A.1) it will be shown that the instantaneous phase of the received signal is as in (A.9). In the derivation is is assumed that $2\pi f_{\mathrm{m}} \tau_{\max}$ is small compared to 2π, where f_{m} is the modulation frequency and $\tau_{\max}$ is the largest group delay caused by the channel.

A discrete equivalent-baseband channel response $\tilde{h}(t)$ is assumed as

$$\tilde{h}(t) = \sum_i a_i \delta(t - \tau_i), \qquad a_i \in \mathbb{C}, \tag{A.1}$$

where a_i is the complex amplitude and τ_i is the group delay for each ray.

The signal to transmit $s_{\mathrm{T}}(t)$ is phase modulated with a given RF amplitude A_{c} and modulated phase $\theta(t)$. Therefore, the equivalent-baseband representation is

$$\tilde{s}_{\mathrm{T}}(t) = A_{\mathrm{c}} e^{\mathrm{j}\theta(t)}. \tag{A.2}$$

The received equivalent-baseband signal $\tilde{s}_{\mathrm{R}}(t)$ is the convolution of the transmitted equivalent-baseband signal with the equivalent-baseband channel

$$\tilde{s}_{\mathrm{R}}(t) = A_{\mathrm{c}} \sum_i a_i e^{\mathrm{j}\theta(t-\tau_i)}. \tag{A.3}$$

As the modulated phase $\theta(t)$ is LF, and only short delays are introduced by the channel, the received signal has a very small phase difference due to the channel. E.g. 25 kHz gives 40 μs $>>$100-ns delay spread. By analysing the instantaneous phase of the modulation and the instantaneous phase difference caused by the channel separately, (A.3) can be linearised

$$\begin{aligned}\tilde{s}_{\mathrm{R}}(t) &= A_{\mathrm{c}} e^{\mathrm{j}\theta(t)} \sum_i a_i e^{\mathrm{j}\theta(t-\tau_i)-\mathrm{j}\theta(t)} \\ &\approx A_{\mathrm{c}} e^{\mathrm{j}\theta(t)} \sum_i a_i \left[1 + \mathrm{j}\theta(t-\tau_i) - \mathrm{j}\theta(t)\right],\end{aligned} \tag{A.4}$$

where $[1+\mathrm{j}\theta(t-\tau_1)-\mathrm{j}\theta(t)]$ is the first-order Taylor expansion of exp($\mathrm{j}\theta(t-\tau_i)-\mathrm{j}\theta(t)$).

The sum over all a_i can be extracted from the summation by introducing

$$A = \sum_i a_i, \qquad A \in \mathbb{C}, \tag{A.5}$$

$$\tilde{s}_R(t) = A_{\mathrm{c}} e^{\mathrm{j}\theta(t)} A \left[1 + \mathrm{j} \sum_i \frac{\theta(t-\tau_i) - \theta(t)}{A} a_i\right]. \tag{A.6}$$

The contributions to the magnitude within the summation is dominated by the 1 term as the phase difference is very small, except if A becomes very small. The total complex magnitude A is only very small if there are signals of equal strength but opposite sign or if there are no strong signals. Therefore, if the LOS is dominant A will not be small. The overall magnitude of the received signal $|\tilde{s_R}|$, assuming a strong LOS is

$$|\tilde{s_R}| \approx A_{\mathrm{c}} |A|. \tag{A.7}$$

As the phase difference variations are very small compared to 2π, the tangent can be linearised

$$\begin{aligned}\arg\left\{1 + \mathrm{j}\frac{\theta(t-\tau_i)-\theta(t)}{A} a_i\right\} &= \operatorname{atan}\left(\frac{\big(\theta(t-\tau_i)-\theta(t)\big)\,\mathbb{R}\mathrm{e}\left\{\frac{a_i}{A}\right\}}{1-\big(\theta(t-\tau_i)-\theta(t)\big)\,\mathbb{I}\mathrm{m}\left\{\frac{a_i}{A}\right\}}\right) \\ &\approx \operatorname{atan}\left(\big(\theta(t-\tau_i)-\theta(t)\big)\,\mathbb{R}\mathrm{e}\left\{\frac{a_i}{A}\right\}\right) \\ &\approx \big(\theta(t-\tau_i)-\theta(t)\big)\,\mathbb{R}\mathrm{e}\left\{\frac{a_i}{A}\right\}.\end{aligned} \tag{A.8}$$

So the overall phase becomes

$$\begin{aligned}\arg\left\{\tilde{s}_{\mathrm{R}}(t)\right\} &= \theta(t) + \arg\{A\} + \sum_i \big(\theta(t-\tau_i) - \theta(t)\big)\,\mathbb{R}\mathrm{e}\left\{\frac{a_i}{A}\right\} \\ &= \arg\{A\} + \sum_i \theta(t-\tau_i)\,\mathbb{R}\mathrm{e}\left\{\frac{a_i}{A}\right\}. \end{aligned} \tag{A.9}$$

A.2 Continuous-time channel impulse response effect on phase estimate

In this section the influence of a continuous-time channel is derived, equivalently to the discrete-ray case in the previous section. Please note that Section A.1 can have rays at any time, and is in that sense continuous, but only has discrete contributions at certain delay times.

Lets assume a continuous equivalent-baseband channel response $\tilde{h}(t)$, where the discrete a_i contributions are replaced by a continuous function $\tilde{h}(t)$, and the delay support $\tau_{\max}$ satisfies $2\pi f_{\mathrm{m}}\tau_{\max} << 2\pi$. Then the received equivalent-baseband signal $\tilde{s}_{\mathrm{R}}(t)$ will be

$$\tilde{s}_{\mathrm{R}}(t) = \int \tilde{h}(\tau) A_{\mathrm{c}} e^{\mathrm{j}\theta(t-\tau)} \mathrm{d}\tau. \tag{A.10}$$

In (A.4) it was assumed that the phase difference caused by the channel is small. As a consequence the amplitude is dominated by the $+1$ term. Therefore, the magnitude is

$$\tilde{s}_{\mathrm{R}}(t) \approx A_{\mathrm{c}} e^{\mathrm{j}\theta(t)} \int \tilde{h}(\tau)\big[1 + \mathrm{j}\theta(t-\tau) - \mathrm{j}\theta(t)\big]\mathrm{d}\tau. \tag{A.11}$$

The integral over $\tilde{h}(\tau)$ can be extracted from the integral by taking

$$\tilde{H}(0) = \int \tilde{h}(\tau)\mathrm{d}\tau, \qquad \tilde{h}(\tau) \in \mathbb{C}, \tag{A.12}$$

where $\tilde{H}(f)$ is the baseband-equivalent Fourier transform of $\tilde{h}(t)$.

The received equivalent-baseband signal can now be reformulated as

$$\tilde{s}_{\mathrm{R}}(t) = A_{\mathrm{c}} e^{\mathrm{j}\theta(t)} \tilde{H}(0) \left\{1 + \frac{\mathrm{j}}{\tilde{H}(0)} \int \tilde{h}(\tau)\left[\theta(t-\tau) - \theta(t)\right]\mathrm{d}\tau\right\}. \tag{A.13}$$

Equivalently to (A.7), provided the phase difference caused by the channel is small. So the magnitude is

$$|\tilde{s}_{\mathrm{R}}(t)| \approx A_{\mathrm{c}} \left|\tilde{H}(0)\right|. \tag{A.14}$$

Equivalently to (A.8) and (A.9) the phase of (A.13) is,

$$\begin{aligned}\hat{\theta}(t) &= \arg\left\{\tilde{s}_{\mathrm{R}}(t)\right\} \\ &\approx \arg\left\{\tilde{H}(0)\right\} + \int \theta(t-\tau)\,\mathbb{R}\mathrm{e}\left\{\frac{\tilde{h}(\tau)}{\tilde{H}(0)}\right\}\mathrm{d}\tau. \end{aligned} \tag{A.15}$$

A.3 Channel impulse response & noise effect on distance estimate

This section will use the influence of the propagation channel (as derived in Section A.2) and AWGN to describe the distance estimations. The derivation is under the assumption of a large SNR and the work is only valid under the condition that $2\pi f_{\mathrm{m}}\tau_{\max} << 2\pi$, where $\tau_{\max}$ is is the largest delay supported by the channel.

Under high SNR the AWGN contribution can be decomposed into a part influencing the received signal amplitude and a part which is orthogonal and thereby influences the phase. Assuming a noise spectral density of $N_0/2$ and applying the properties of bandpass processes from [8] it can be shown that the noise spectral density influencing the received signal phase $S_{N_{\mathrm{Q}}}(f)$ is

$$S_{N_{\mathrm{Q}}}(f) = N_0. \tag{A.16}$$

From the received signal the estimated phase $\hat{\theta}(t)$ is given by (A.15) plus the AWGN contribution. The noise contribution is added to the received signal, the phase offset created is $\tan(N_{\mathrm{Q}}/|\tilde{s}_{\mathrm{R}}|)$. For large SNR the tangent can be linearised as $\tan x = x$. So the estimated phase is

$$\hat{\theta}(t) = \arg\left\{\tilde{H}(0)\right\} + \int \mathbb{Re}\left\{\frac{\tilde{h}(\tau)}{\tilde{H}(0)}\right\}\theta(t-\tau)\mathrm{d}\tau + \frac{N_{\mathrm{Q}}(t)}{A_{\mathrm{c}}\left|\tilde{H}(0)\right|}. \tag{A.17}$$

Assuming a sinusoidal modulating signal, $\theta(t) = A_{\mathrm{m}}\cos(2\pi f_{\mathrm{m}} t)$, where A_{m} is the modulation amplitude and f_{m} is the modulating frequency

$$\hat{\theta}(t) = \arg\left\{\tilde{H}(0)\right\} + A_{\mathrm{m}}\int \mathbb{Re}\left\{\frac{\tilde{h}(\tau)}{\tilde{H}(0)}\right\}\cos\left(2\pi f_{\mathrm{m}}(t-\tau)\right)\mathrm{d}\tau + \frac{N_{\mathrm{Q}}(t)}{A_{\mathrm{c}}\left|\tilde{H}(0)\right|}. \tag{A.18}$$

To find the instantaneous phase difference between the transmitted and received signals, a reference signal is used with a $\pi/2$ phase offset. Multiplying the reference and received signals one gets the sine of the sum and difference of the beforementioned signals. The difference term contains the phase difference. The sum term can be filtered out because it is at double the frequency. Therefore, the phase difference between the reference and the received signal is found by multiplication followed by an integrate and dump operation over an integer number of modulation periods. This results in a phase difference

$$\Delta\hat{\phi}_{\mathrm{m}} = \frac{2}{A_{\mathrm{m}}T_{\mathrm{s}}}\int_0^{T_{\mathrm{s}}} \hat{\theta}(t)\sin(2\pi f_{\mathrm{m}} t)dt, \quad T_{\mathrm{s}} = N/f_{\mathrm{m}}, \quad N \in \{1, 2, \ldots\}, \tag{A.19}$$

where T_s is the integration or symbol time.

The angle difference identity can be used to separate the time-dependent and lag-dependent contributions to the phase signal $\hat{\theta}(t)$

$$\cos\left(2\pi f_\mathrm{m}(t-\tau)\right) = \cos(2\pi f_\mathrm{m} t)\cos(2\pi f_\mathrm{m}\tau) + \sin(2\pi f_\mathrm{m} t)\sin(2\pi f_\mathrm{m}\tau), \tag{A.20}$$

and with product identities for $\cos(2\pi f_\mathrm{m} t)\cdot\sin(2\pi f_\mathrm{m} t)$ and $\sin(2\pi f_\mathrm{m} t)\cdot\sin(2\pi f_\mathrm{m} t)$ it can be shown that

$$\Delta\hat{\phi}_\mathrm{m} = \int \mathbb{R}\mathrm{e}\left\{\frac{\tilde{h}(\tau)}{\tilde{H}(0)}\right\}\sin\left(2\pi f_\mathrm{m}\tau\right)\mathrm{d}\tau + N_{\Delta\phi}, \tag{A.21}$$

$$N_{\Delta\phi} = \frac{2}{A_\mathrm{m} T_\mathrm{s} A_\mathrm{c}|\tilde{H}(0)|}\int_0^{T_\mathrm{s}} N_\mathrm{Q}(t)\sin(2\pi f_\mathrm{m} t)dt. \tag{A.22}$$

As $2\pi f_\mathrm{m}\tau_\mathrm{rms} << 2\pi$ is assumed the sine can be linearised. Therefore,

$$\Delta\hat{\phi}_\mathrm{m} \approx \int \mathbb{R}\mathrm{e}\left\{\frac{\tilde{h}(\tau)}{\tilde{H}(0)}\right\} 2\pi f_\mathrm{m}\tau\mathrm{d}\tau + N_{\Delta\phi}. \tag{A.23}$$

The variance of the noise after detection is a scaled version of the variance before detection N_0 as only linear operations are preformed. Therefore,

$$\sigma^2_{N_{\Delta\phi}} = \frac{2N_0}{A_m^2 A_c^2 |\tilde{H}(0)|^2 T_\mathrm{s}}. \tag{A.24}$$

The estimated distance $\hat{d}$ can be calculated from the detected phase estimate

$$\hat{d} = \frac{c_0\Delta\hat{\phi}_\mathrm{m}}{4\pi f_\mathrm{m}} = \frac{c_0}{2}\int \mathbb{R}\mathrm{e}\left\{\frac{\tilde{h}(\tau)}{\tilde{H}(0)}\right\}\tau\mathrm{d}\tau + d_\mathrm{n}, \tag{A.25}$$

$$d_\mathrm{n} = \frac{c_0}{4\pi f_\mathrm{m}}\frac{2}{A_\mathrm{m} T_\mathrm{s} A_\mathrm{c}|\tilde{H}(0)|}\int_0^{T_\mathrm{s}} N_\mathrm{Q}(t)\sin(2\pi f_\mathrm{m} t)dt, \tag{A.26}$$

where c_0 is the speed of light in vacuum.

The variance of the noise on the distance estimate is again scaled, such that

$$\sigma^2_{d_n} = \frac{c_0^2 N_0}{8\pi^2 f_\mathrm{m}^2 A_\mathrm{m}^2 A_\mathrm{c}^2 |\tilde{H}(0)|^2 T_\mathrm{s}}. \tag{A.27}$$

An interesting observation is that

$$E_\mathrm{s} = \frac{1}{2}A_\mathrm{c}^2|\tilde{H}(0)|^2 T_\mathrm{s}. \tag{A.28}$$

With this the variance of the noise can be expressed more elegantly as

$$\sigma^2_{d_n} = \frac{c_0^2}{4\pi^2 f_\mathrm{m}^2 A_\mathrm{m}^2 E_\mathrm{s}/N_0}. \tag{A.29}$$

A.4 Stochastic model for the distance estimate in line of sight scenario

In this section the result of Section A.3 is applied to a strong LOS scenario assuming US.

The channel response $\tilde{h}(\tau)$ will be assumed to have a LOS component

$$\tilde{h}(\tau) = a_{\mathrm{LOS}}\delta(\tau - \tau_{\mathrm{los}}) + \tilde{h}_{\mathrm{MPC}}(\tau), \tag{A.30}$$

where a_{LOS} is the complex amplitude for the LOS and $\tilde{h}_{MPC}(\tau)$ is the complex response for the MPs.

$\tilde{h}_{\mathrm{MPC}}(\tau)$ is assumed to consist of US. Therefore, the ACF of the MPs is

$$R_{h_{\mathrm{MPC}}}(\tau, \tau') = \mathrm{E}\left[\tilde{h}^*_{\mathrm{MPC}}(\tau)\tilde{h}_{\mathrm{MPC}}(\tau')\right] = P_{\mathrm{MPC}}(\tau)\delta(\tau - \tau'), \tag{A.31}$$

where $\mathrm{E}[\cdot]$ is the expected value and $P_{\mathrm{MPC}}(\tau)$ is the PDP.

Therefore, the expected value of the complex amplitude $\tilde{H}(0)$, equivalent to (A.12), is

$$\mathrm{E}[\tilde{H}(0)] = \mathrm{E}\left[a_{\mathrm{LOS}} + \int \tilde{h}_{\mathrm{MPC}}(\tau)\mathrm{d}\tau\right] = a_{\mathrm{LOS}}. \tag{A.32}$$

And $\tilde{H}(0)$ has a variance of,

$$\begin{aligned}
\mathrm{E}[|\tilde{H}(0)|^2] &= |a_{\mathrm{LOS}}|^2 + \iint P_{\mathrm{MPC}}(\tau)\delta(\tau - \tau')\mathrm{d}\tau\mathrm{d}\tau', && \text{(A.33)}\\
&= |a_{\mathrm{LOS}}|^2 + P_{\mathrm{MPC}}, && \text{(A.34)}\\
&= |a_{\mathrm{LOS}}|^2 \frac{1+K}{K}, && \text{(A.35)}
\end{aligned}$$

where $P_{\mathrm{MPC}} = \int P_{\mathrm{MPC}}(\tau)\mathrm{d}\tau$ and $K = |a_{\mathrm{LOS}}|^2/P_{\mathrm{MPC}} = P_{\mathrm{LOS}}/P_{\mathrm{MPC}}$, which is the scaling factor K in Rician fading.

The distance estimate, starting from (A.25), can be reformulated to show the contributions from the LOS, MPs and AWGN:

$$\begin{aligned}
\hat{d} &= \frac{c_0}{2}\int \mathbb{R}\mathrm{e}\left\{\frac{1}{\tilde{H}(0)}\left[a_{\mathrm{LOS}}\delta(\tau - \tau_{\mathrm{LOS}}) + \tilde{h}_{\mathrm{MPC}}(\tau)\right]\right\}\tau\mathrm{d}\tau + d_{\mathrm{n}}\\
&= \frac{c_0}{2}\mathbb{R}\mathrm{e}\left\{\frac{a_{\mathrm{LOS}}}{\tilde{H}(0)}\right\}\tau_{\mathrm{LOS}} + \frac{c_0}{2}\int \mathbb{R}\mathrm{e}\left\{\frac{\tilde{h}_{\mathrm{MPC}}(\tau)}{\tilde{H}(0)}\right\}\tau\mathrm{d}\tau + d_{\mathrm{n}}\\
&= \frac{c_0}{2}\tau_{\mathrm{LOS}} - \frac{c_0}{2}\tau_{\mathrm{LOS}}\int \mathbb{R}\mathrm{e}\left\{\frac{\tilde{h}_{\mathrm{MPC}}(\tau)}{\tilde{H}(0)}\right\}\mathrm{d}\tau + \frac{c_0}{2}\int \mathbb{R}\mathrm{e}\left\{\frac{\tilde{h}_{\mathrm{MPC}}(\tau)}{\tilde{H}(0)}\right\}\tau\mathrm{d}\tau + d_{\mathrm{n}}. && \text{(A.36)}
\end{aligned}$$

Such that,

$$\hat{d} = d + d_{\mathrm{h}} + d_{\mathrm{n}}, \tag{A.37}$$

$$d = \frac{c_0}{2}\tau_{\mathrm{LOS}}, \tag{A.38}$$

$$d_{\mathrm{h}} = \frac{c_0}{2}\int \mathbb{R}\mathrm{e}\left\{\frac{\tilde{h}_{\mathrm{MPC}}(\tau)}{\tilde{H}(0)}\right\}(\tau - \tau_{\mathrm{LOS}})\mathrm{d}\tau, \tag{A.39}$$

$$d_{\mathrm{n}} \sim \mathcal{N}\left(0, \frac{c_0^2 N_0}{8\pi^2 f_{\mathrm{m}}^2 A_{\mathrm{m}}^2 A_{\mathrm{c}}^2 |\tilde{H}(0)|^2 T_{\mathrm{s}}}\right), \tag{A.40}$$

where $\mathcal{N}(\mu, \sigma^2)$ is a Gaussian distribution, with mean μ and variance σ^2, for the noise.

Given a strong LOS, $K >> 1$, (A.35) becomes almost deterministic,

$$|\hat{H}(0)|^2 \approx P_{\mathrm{LOS}}. \tag{A.41}$$

Therefore, d_{h} is only random in $\tilde{h}_{\mathrm{MPC}}(\tau)$. As $\tilde{h}_{\mathrm{MPC}}(\tau)$ is Gaussian and only linear operations on this Gaussian are assumed, d_{h} will be Gaussian with $\mathrm{E}[d_{\mathrm{h}}] = 0$ and a variance

$$\begin{aligned}
\sigma_{d_{\mathrm{h}}}^2 &= \mathrm{E}\left[d_{\mathrm{h}}^2\right] \\
&= \frac{c_0^2}{16}\mathrm{E}\Bigg\{\iint \left[\frac{\tilde{h}_{\mathrm{MPC}}(\tau)}{\tilde{H}(0)} + \frac{\tilde{h}_{\mathrm{MPC}}^*(\tau)}{\tilde{H}^*(0)}\right]\left[\frac{\tilde{h}_{\mathrm{MPC}}(\tau')}{\tilde{H}(0)} + \frac{\tilde{h}_{\mathrm{MPC}}^*(\tau')}{\tilde{H}^*(0)}\right] \\
&\qquad\qquad \cdot (\tau - \tau_{\mathrm{LOS}})(\tau' - \tau_{\mathrm{LOS}})\mathrm{d}\tau\mathrm{d}\tau'\Bigg\} \\
&= \frac{c_0^2}{8}\iint \frac{1}{|\tilde{H}(0)|^2}\mathbb{R}\mathrm{e}\left\{\mathrm{E}\left[\tilde{h}_{\mathrm{MPC}}(\tau)\tilde{h}_{\mathrm{MPC}}^*(\tau')\right]\right\}(\tau - \tau_{\mathrm{LOS}})(\tau' - \tau_{\mathrm{LOS}})\mathrm{d}\tau\mathrm{d}\tau' \\
&= \frac{c_0^2}{8}\frac{1}{|\tilde{H}(0)|^2}\int P_{\mathrm{MPC}}(\tau)(\tau - \tau_{\mathrm{LOS}})^2\mathrm{d}\tau \\
&= \frac{c_0^2}{8P_{\mathrm{LOS}}}P_{\mathrm{MPC}}(\sigma_{\tau,\mathrm{dif}}^2 + T_{\mathrm{m,dif}}^2) \\
&= \frac{c_0^2(\sigma_{\tau,\mathrm{dif}}^2 + T_{\mathrm{m,dif}}^2)}{8K},
\end{aligned} \tag{A.42}$$

where $\sigma_{\tau,\mathrm{dif}}$ is the RMS delay spread of the diffuse part of the channel and $T_{\mathrm{m,dif}}$ is the mean excess delay of the diffuse part of the channel

$$T_{\mathrm{m,dif}} = \frac{1}{P_{\mathrm{MPC}}}\int P_{\mathrm{MPC}}(\tau)(\tau - \tau_{\mathrm{LOS}})\mathrm{d}\tau. \tag{A.43}$$

For an exponential PDP the mean excess delay is equal to the RMS delay spread, $T_{\mathrm{m,dif}} = \sigma_{\tau,\mathrm{dif}}$.

Therefore, the distance estimate $\hat{d}$ is a Gaussian random variable (RV) with $\mathrm{E}[\hat{d}] = d$ (unbiased) and a variance which is the sum of (A.42) and (A.27)

$$\begin{aligned}\sigma_{\mathrm{d}}^2 &= \sigma_{\mathrm{d_h}}^2 + \sigma_{\mathrm{d_n}}^2 \\ &= \frac{c_0^2(\sigma_\tau^2 + T_{\mathrm{m,dif}}^2)}{8K} + \frac{c_0^2 N_0}{8\pi^2 f_{\mathrm{m}}^2 A_{\mathrm{m}}^2 A_{\mathrm{c}}^2 |a_{\mathrm{LOS}}|^2 T_{\mathrm{s}}} \\ &= \frac{c_0^2}{4}\left[\frac{\sigma_{\tau,\mathrm{dif}}^2 + T_{\mathrm{m,dif}}^2}{2K} + \frac{1}{4\pi^2 f_{\mathrm{m}}^2 A_{\mathrm{m}}^2 E_{\mathrm{s}}/N_0}\right],, \end{aligned} \tag{A.44}$$

where E_{s} is the symbol energy,

$$E_{\mathrm{s}} = \frac{1}{2} A_{\mathrm{c}}^2 |a_{\mathrm{LOS}}|^2 T_{\mathrm{s}}. \tag{A.45}$$

Assuming GMSK modulation which uses a triangular $\theta(t)$, the same analysis stays valid. However f_{m} and A_{m} become functions of the bit time T_{b} and number of bits per symbol N_{b}. The modulation frequency is $f_{\mathrm{m}} = 1/(T_{\mathrm{b}} N_{\mathrm{b}})$ and the amplitude is $A_{\mathrm{m}} = N_{\mathrm{b}}/(4T_{\mathrm{b}})$. The modulation amplitude A_{m} is reduced to the power in the first harmonic by the Gaussian filter. So the effective modulation amplitude
$A_{\mathrm{m0}} = 8/\pi^2 A_{\mathrm{m}}$. This simplifies (A.44) to

$$\sigma_{\mathrm{d}}^2 = c_0^2\left[\frac{\sigma_{\tau,\mathrm{dif}}^2 + T_{\mathrm{m,dif}}^2}{8K} + \frac{T_{\mathrm{b}}^2}{16 E_{\mathrm{s}}/N_0}\right] \tag{A.46}$$

The detection in the target will make the same error as it has no additional information. If the return signal is sent through the same channel the error due to the channel (d_{h}) is doubled so the variance becomes 4 times larger. i.e,

$$\sigma_{\mathrm{d}}^2 = c_0^2\left[\frac{\sigma_{\tau,\mathrm{dif}}^2 + T_{\mathrm{m,dif}}^2}{2K} + \frac{T_{\mathrm{b}}^2}{16 E_{\mathrm{s}}/N_0}\right] \tag{A.47}$$

Appendix B

Table of conditions

Table B.1: Overview of conditions applied of reported work.

Num.	Sec.	Condition
1	2.4	The round-trip distance should be small compared to $c/(2f_\mathrm{m})$.
2	2.5	The target node introduces no error to the signal.
3	2.5	The noise power at the detector input is small compared to the RF carrier power $A_\mathrm{c}^2/2$.
4	3.2	The phase shift caused by the excess delays of MPs is small, $2\pi f_\mathrm{m}\tau_{ex} << 2\pi$.
5	3.3.1	The channel is US and quasi static.
6	3.3.2	There must be a dominant component in the channel for the ranging method to work.
7	3.3.3	The channel has a dense exponential PDP.
8	3.4	There must be a strong LOS $K >> 1$ for the MP channel impact to be Gaussian.
9	4.4.1	The two-tap simulation model requires $\sigma_\tau << \Delta T$.

Appendix C

BLE communication SNR and distance indication

From the BLE specifications it follows that for communication the bit error probability P_r shall be $\leq$0.1%. Note that the bit error probability has no direct meaning for ranging, as it is an estimation problem, not a detection problem. However the SNR relation to P_r can be used. The SNR per bit SNR_b for the stated worst case P_r is

$$P_\mathrm{r} = Q\left(\sqrt{\frac{E_\mathrm{b}}{N_0}}\right), \tag{C.1}$$

$$SNR_\mathrm{b} = \frac{E_\mathrm{b}}{N_0} = \left(Q^{-1}(P_\mathrm{r})\right)^2 \approx 9.5, \tag{C.2}$$

$$SNR_\mathrm{b,dB} \approx 9.8, \tag{C.3}$$

where $Q(\cdot)$ is the Q-function. For perfect coherent detection of the MSK.

In [1] it is shown that for ranging, with a MSE of 0.25 m^2 or less, an SNR per symbol is needed of 44 dB or more. Therefore, with the worst case SNR per bit for communication it can be seen that a symbol time T_s is needed of

$$T_\mathrm{s} = \frac{E_\mathrm{s}/N_0}{E_\mathrm{b}/N_0} T_\mathrm{b} = 2.6 \cdot 10^{-3}\ \mathrm{s}, \tag{C.4}$$

where the SNRs are linear.

An indication of the maximum distance d_max can be calculated using Friis equation. If unit directivity is assumed and the BLE power specifications from [5] are used, as shown in Table C.1, then the maximum distance is

$$d_\mathrm{max} = \frac{4\pi}{\lambda}\sqrt{\frac{P_\mathrm{T} D_\mathrm{T} D_\mathrm{R}}{P_\mathrm{R}}} \approx 315, \tag{C.5}$$

where λ is the carrier wave length, D_T is the transmit antenna directivity, D_R is the receive antenna directivity, $P_\mathrm{T,max}$ is the maximum power output (linear) and P_R is the receiver sensitivity (linear). Note that this is effectively a best case scenario, as no fading margin, feeder losses and other limiting factors are considered.

If, for arguments sake, there are fading effects, causing a path loss exponent of 3, then the maximum distance would reduce to just under 10 m. Note, this is a very limited scenario as other contributions to a real link budget analysis are not taken into account.

Table C.1: BLE power and bit error probability specifications

BLE parameters	**Symbol**	**Value range**
Bit error probability	P_{r}	$<$ 0.01%
Max. transmission power	$P_{\mathrm{T,dB,max}}$	20 dBm
Receiver sensitivity	$P_{\mathrm{R,dB}}$	-70 dBm

Appendix D

Cumulative distribution functions

This appendix contains the CDFs for various scenarios presented in Chapter 5. In Section D.1 the CDFs for different σ_τ, K and E_s/N_0 are presented corresponding to the experiments in Section 5.3. Section D.2 contains the CDFs of three of the experiments presented in Section 5.4, these are the results for only AWGN, only MPs and the two combined.

D.1 Experiment in Figure 5.4

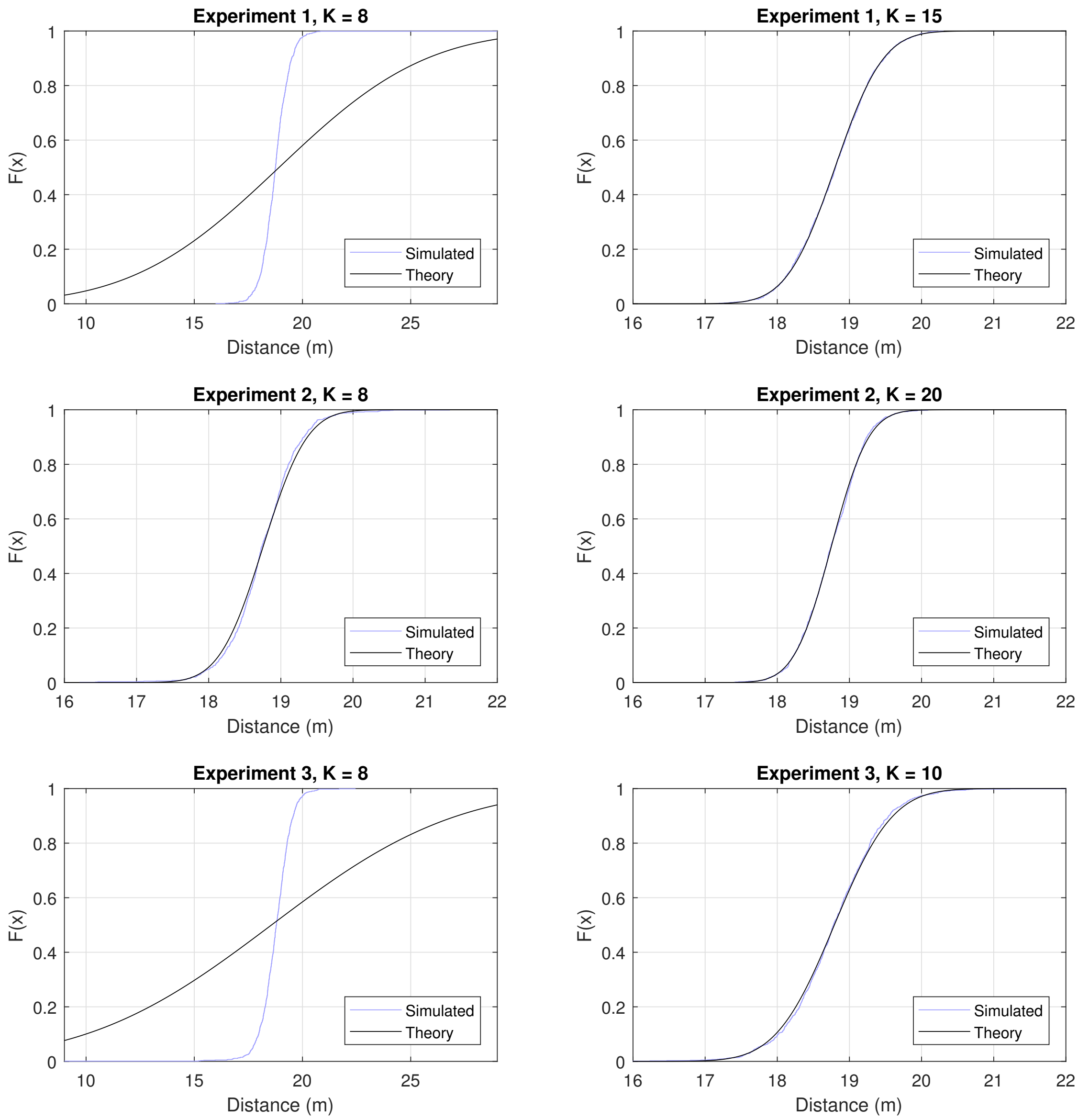

Figure D.1: Selection of CDFs from experiments in Figure 5.4.

D.2 Experiment in Figure 5.6

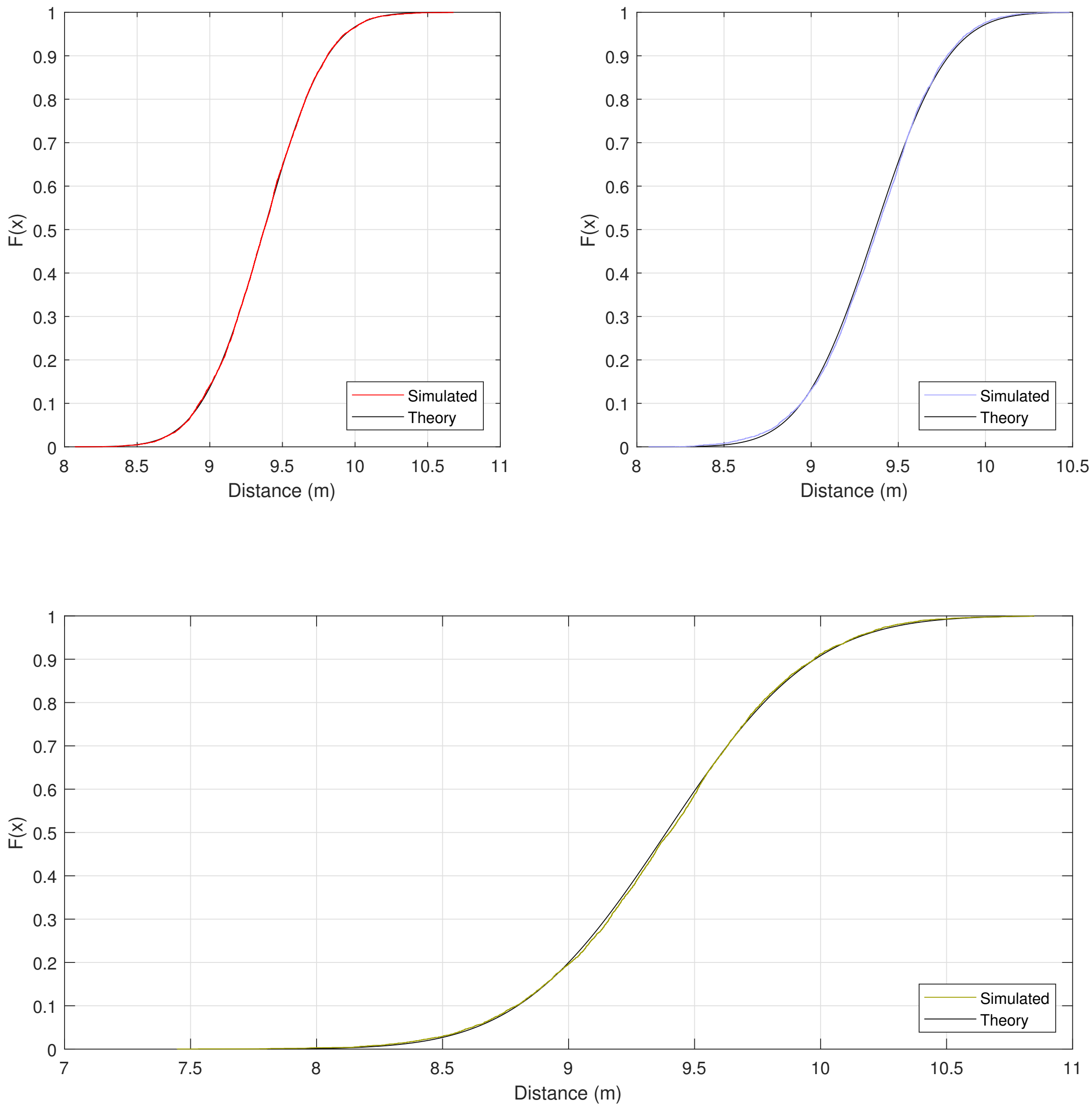

Figure D.2: CDF of experiments in Figure 5.6. **Top left:** Noise experiment. **Top right:** MP experiment. **Bottom:** Total experiment.